IEEE Access
Multidisciplinary | Rapid Review | Open Access Journal

Received June 18, 2021, accepted July 13, 2021, date of publication July 27, 2021, date of current version August 12, 2021.

Digital Object Identifier 10.1109/ACCESS.2021.3100700

Review of the State-of-the-Art of Brain-Controlled Vehicles

AMIN HEKMATMANESH[1], PEDRO H. J. NARDELLI[2], (Senior Member, IEEE), AND HEIKKI HANDROOS[1], (Member, IEEE)

[1]Laboratory of Intelligent Machines, LUT University, 53850 Lappeenranta, Finland
[2]School of Energy Systems, LUT University, 53850 Lappeenranta, Finland

Corresponding author: Amin Hekmatmanesh (amin.hekmatmanesh@lut.fi)

ABSTRACT Brain-Controlled Vehicle (BCV) is an already established technology usually designed for disabled patients. This review focuses on the most relevant topics on brain-controlled vehicles, with a special reference to the terrestrial BCV (e.g., the mobile car, car simulator, real car, graphical and gaming car) and the aerial BCV, also called BCAV (e.g., real quadcopters, drones, fixed wings, graphical helicopter, and aircraft) controlled by using bio-signals, such as electroencephalogram (EEG), Electrooculogram (EOG), and Electromyogram (EMG). For instance, EEG-based algorithms detect patterns from the motor imaginary cortex area of the brain for intention detection, patterns like event-related desynchronization/event-related synchronization, steady-state visually evoked potentials, P300, and generated local evoked potential patterns. We have identified that the reported best-performing approaches employ machine learning and artificial intelligence optimization methods, namely support vector machine, neural network, linear discriminant analysis, k-nearest neighbor, k-means, water drop optimization, and chaotic tug of war. We considered the following metrics to analyze the efficiency of the different methods: type and combination of bio-signals, time response, and accuracy values with statistical analysis. The present work provides an extensive literature review of the key findings of the past ten years, indicating future perspectives in the field.

INDEX TERMS Bio-signal patterns, control, machine learning, artificial intelligence simulator, vehicle, aerial vehicle.

NOMENCLATURE

BCA	Brain-Controlled Aerial Vehicle
BCI	Brain Computer Interface
BCV	Brain-Controlled Vehicle
CCA	Canonical Correlation Analysis
CI-CSP	Complete Information Common Spatial Pattern
CNN	Convolutional Neural Network
CSP	Common Spatial Pattern
CTWO	Chaotic Tug of War Optimization
DFA	Detrended Fluctuation Analysis
DSLVQ	Sensitive Learning Vector Quantization
DT	Decision Tree
EBC	Emergency Brakes Control
EEG	Electroencephalogram
EMG	Electromyogram
EOG	Electrooculogram
EP	Evoke Potential
ERD	Event-Related Desynchronization
ERP	Event-Related Potentials
ERS	Event-Related Synchronization
FBCCA	Filter Bank Canonical Correlation Analysis
fMRI	functional magnetic resonance imaging
FN	False Negative
fNIRS	functional Near-Infrared Spectroscopy
FP	False Positive
GGAP	Generalized Growing and Pruning
GHMM	Gaussian mixture-hidden Markov model
GMM	Gaussian Mixture Model
GPS	Global Positioning System
GRBF	Generalized RBF
HbO	Oxy-hemoglobin
HbR	Deoxy-hemoglobin
HMD	Head-Mounted Device

The associate editor coordinating the review of this manuscript and approving it for publication was Jad Nasreddine.

HMM	Hidden Markov Model
HUD	Head-Up Display
ICA	Independent Component Analysis
IM	Imaginary Movement
K-NN	K-Nearest Neighbor
LDA	Linear Discriminant Analysis
LEP	Localized Evoked potential
LR	Logistic Regression
MPC	Model Predictive Control
NN	Neural Network
OAC	Obstacle Avoidance Control
PCA	Principal Component Analysis
PSD	Power spectrum Density
QN	Queuing Network
RBF	Radial Basis Function
RBFNN	Radial Basis Function Neural Network
RLDA	Regularized Linear Discriminant Analysis
RP	Readiness Potentials
SCS	Shared Control Strategy
semi-MIM	Semi-Supervised Mutual Information Maximization
SMSVM	Soft Margin SVM
SNR	Signal-to-Noise Ratio
SSVEP	Steady-State Visually Evoked Potential
SVM	Support Vector Machine
TN	True Negative
TP	True Positive
TSVM	Transductive Support Vector Machine
VPA	Vector Phase Analysis
WDO	Water Drop Optimization

I. INTRODUCTION

The recent research in neuroscience supported by the development of high-precision sensors and artificial intelligence methods has significantly increased our knowledge about how the human brain works. In particular, human body movements activate neurons in the sensorimotor cortex area. The activated neurons generate action potentials for different actions, which have different patterns with specific properties. Several studies have been conducted to explore patterns in electroencephalogram (EEG) signals. The patterns would be related to voluntary movements or the human body reaction based on the condition, such as stress that our recent review paper on stress detection for drivers and heavy equipment operators considered this phenomena comprehensively [1]. Subsequently, automatic methods of identifying and predicting these patterns specifically at the onset of a voluntary movement have been introduced [2].

The Brain Computer Interface (BCI) science uses the patterns in EEG signals for the control of applications, such as bionic hands [3], [4], ankle foot orthosis [5], [6], mobile robots [7], vehicles [8], and wheelchair [9]–[11]. These applications are useful for disabled people, who could potentially enjoy a more convenient life. Among the vast variety of BCI applications, this review focuses on the Brain-Controlled Vehicle (BCV) and the Brain-Controlled Aerial Vehicle (BCAV), mainly designed for non-disabled people and in particular for those not having suffered a brain stroke. The benefits of BCV and BCAV applications for skilled workers are for instance easier and faster execution of various tasks, relatively low costs of missions, precision in hazardous missions, remote access to remote locations and research targets, such as safety checks of large areas, burned areas, provision of first-aid equipment in accidents in remote locations, and acquisition of weather information from areas that are difficult to access (mountains, pole areas, or volcanoes). Figs. 1 to 3 illustrate BCV and BCAV applications, respectively.

In particular, the BCV aims at tasks related to car navigation, viz. keeping the lane, passing and following cars, turning, Obstacle Avoidance Control (OAC), and braking in different situations, specifically the Emergency Brakes Control (EBC). The same commands are computed for the BCAV with two more directions of moving upward (take-off) and downward (landing). In general, the control of a BCAV application is more challenging.

One of the most important bio-signals is the EEG, where the first step is to know the EEG rhythms and changes after tasks and stimulation. The important patterns to diagnose the intentions of drivers are Event-Related Potentials (ERPs), Steady-State Visually Evoked Potentials (SSVEP), Desynchronization/ Event Related Synchronization (ERD/ERS), Readiness Potentials (RP), and Local Evoked Potentials (LEP). In the case of an intention of a movement, specific patterns appear in the EEG about 0.5 s to 2 s before the movement, and then, the intention turns into action [12]. The objective in the studies reviewed in this paper has been to develop novel algorithms for finding the onset of Imaginary Movement (IM) patterns, such as ERD/ERS and RP.

Despite its widespread use, the resolution of EEG real-time signals is usually not good enough for BCV and BCAV applications. Therefore, hybrid methods have been developed to overcome the defects of the previous methods. For example, the use of the EEG with other bio-signals, such as Electromyogram (EMG), Electrooculogram (EOG), and functional Near-Infrared Spectroscopy (fNIRS) has been proposed to gain more information of human beings for control applications. In addition to bio-signals, external sensors are deployed for recording and analyzing the information about the environment to facilitate a better analysis of the EEG and the situation.

The aim of the present paper is to provide a comprehensive review of BCV and BCAV studies over the past ten years. Because there is a redundant of the algorithms and applications in published conferences and journals, a selection of papers were performed to avoid repetition. Furthermore, we expect that the present contribution would be helpful to understand the recent history of the field, and how ideas and studies have been developed further and improved. Thus, new

ideas for future developments, based on recent technologies, could be better contextualized. The papers covered in this study are summarized in Tables 1 to 2, presented in Appendix, to provide a systematic comparison between the different contributions.

The rest of this paper is organized as follows: Section II provides the background knowledge, mainly based on brain rhythms with intention identification approaches and a data acquisition model, both applied in the BCV and the BCAV, as well as open questions and limitations of the study. Section III addresses the algorithms for automatically predicting the intention of the drivers based on patterns from bio-signals. Section IV introduces applications for training and testing the models in the real-time mode. Section V concludes the review by presenting the already solved questions and current limitations, while providing our future vision of the topic.

II. BACKGROUND ON BCV

In the following, technologies deployed for recording bio-signals are introduced. In addition, the rhythms related to the control of BCV and BCAV applications are presented.

A. BRAIN RHYTHMS AND PATTERNS FOR THE BCV AND THE BCVA

Brain is an organ composed of neurons that generate different rhythms with specific features. The detectable rhythms change based on the type of action and stimulation. Changes in the rhythms are also a key clue for early diagnosis of a disease and serious health condition. By focusing on the sensorimotor cortex area rhythms it is possible to predict the subject's intention of movement. Some of the patterns studied for intention detection (thinking) are ERD [13], ERP [14], ERS [13], and SSVEP [15], and they are defined as follows.

1) ERD/ERS PATTERN

ERD is a cognitive pattern, which occurs after an intention to move, and ERS is the second pattern, which occurs immediately after the ERD if the intention turns into action. The location where the pattern is recorded is the sensorimotor cortex area of the brain [5].

2) SSVEP PATTERN

The SSVEP is a response pattern, which occurs when a visual stimulation is applied to a human. By applying a visual stimulation in a specific range, the same evoked potential patterns called SSVEP will occur in the visual cortex. The advantages of the SSVEP are the high Signal-to-Noise Ratio (SNR) compared with other patterns [15].

3) ERP PATTERN

ERPs are the measured electrophysiological response by the EEG to a specific stimulation. The P300 ERP is a known brain response to a cognitive event after 300 ms. Some of the other patterns are, e.g., N100, N200, and P100. The P300 is the pattern aimed at in the control applications [13]. For example, the P300 pattern has been used for typing applications (prediction, decision-making) for disabled patients, concentrating on the letters. In BCV applications, the P300 is employed for destination selection.

4) LEP PATTERN

Some studies have focused on searching for new ERPs for better control systems. To this end, new tasks, such as auditory tasks, have been designed and applied to stimulate neurons other than sensorimotor cortex area, and the obtained patterns, named as LEP have been employed for further computations and control applications [16].

5) RP PATTERNS

Readiness Potential (RP) is a pattern generated about 1.5 s to 1 s before a real movement. The RP is associated with repetitive voluntary movements, such as walking. In the processing, the RP is divided into early and late RPs. The early RP occurs about 1.5 s before a voluntary movement in the central area of the cortex, and the late RP about 500 ms before the voluntary movement in the primary motor cortex area [17], [18].

B. DATA ACQUISITION

In order to control a BCI application using bio-signals, amplifiers to measure the human body changes during the experiments are required. Well-known devices are EEG, EMG, EOG amplifiers (suitable for real-time processing), fNIRS, and functional Magnetic Resonance Imaging (fMRI) devices, the details of which are presented as follows:

1) EEG, EMG, AND EOG AMPLIFIERS

To measure noninvasive signals from heart, brain activities, and muscles, ECG, EEG, and EMG amplifiers, respectively, are deployed. The usual electrodes for acquiring EEG, EMG, and ECG signals are the Ag/AgCl, known as nonpolarized electrodes. The other popular electrode is disposable (single-use) electrode, called a gel-based or Bio-Potential (BP) electrode. In theory, the BP electrode senses ion flow on the tissue surface and then converts it into electron current. For the EMG measurement using BP electrodes, the ion distribution is generated by applying nervous stimuli and muscle contraction. The electrodes deployed are categorized as nonpolarized and polarized. The nonpolarized electrodes (Ag/Agcl) pass the current across the electrolyte interface. Thus, less noise is recorded compared with polarized electrodes in the case of movement noise. Furthermore, nonpolarized electrodes are easy to manufacture, and they have a very low half-cell potential termed as dc offset. Therefore, Ag/Agcl electrodes are popular for the EEG recording compared with other electrodes. The polarized electrodes do not let the current move freely across the interface between the electrode and the electrolyte, which acts similar to capacitors.

2) fNIRS

The fNIRS is a noninvasive imaging system for measuring the hemoglobin (Hb) concentration changes in the neurovasculature system of the brain. The Hb concentration changes are measured by optical intensity measurements (characteristic absorption spectra) by near-infrared light. The studies applying the fNIRS are usually hybrid methods with EEG signals for real-time control of the BCVA applications. The fNIRS has been used for the primary motor cortex area for imaginary tasks to determine accurately the areas the brain activity takes place and use them for identification procedures [19].

3) fMRI

The fMRI is an accurate noninvasive imaging system for demonstrating the localized power in a brain map with a high resolution. The mechanism is based on hemodynamic changes of the brain that are associated with neuronal activity [20]. In the present review, the fMRI is employed for the control of BCAV applications. The fMRI is usually employed as a hybrid method with the EEG to obtain significant results in real-time systems.

4) EXTERNAL SENSORS

Hybrid methods are a combination of different signals to improve the significance of the results. In some methods, a combination of different bio-signals with non-bio-signals are used to identify the driver's intention and to navigate accurately, such as a combination of the EEG with the EMG, Global Positioning System (GPS), cameras, fNIRS, google glasses, and motion sensors known as external sensors (e.g., acceleration, velocity, and wind speed) [21], [22].

C. CHALLENGES OF BRAIN SIGNAL PROCESSING

Here, an identification algorithm steps are introduced and the challenges in each step is considered and the details of the algorithm in each step is explained in details in section III. In order to control a vehicle, either by the BCV or the BCAV by using bio-signals, the following main steps are required:

1) preprocessing,
2) feature extraction,
3) optimization (can be applied to features and classifiers)
4) feature selection,
5) classifiers,
6) statistical analysis,
7) real-time experiments.

Fig. 1 provides a description of those steps and possible options to be considered. These options will be described next.

At present, some of the initial BCV EEG-based questions and limitations have been solved; for instance, the area of the cortex for recording the EEG related to specific tasks such as hand movement, the frequency range of neuron activities, and the specific patterns related to the applied stimulation, and how to develop algorithms for automatically finding the patterns.

The unsolved problems are mathematical algorithms for noise rejection and automatic identification of specific patterns with a high precision. In particular, development of effective algorithms for feature extraction and classification for automatic pattern identification are challenging tasks. Further questions associated with neuron connectivity are, for instance: which neurons are connected in a specific task, and how neurons communicate after the stimulation.

Other challenges are related to the mathematical approaches for prediction of patterns, design of real-time algorithms, and speeding up the processing of time-consuming methods, such as wavelet-based methods. The key problems in the BCV applications based on the EEG are (i) the nonlinearity of the brain, generating patterns of different varieties for individual participants; (ii) the denoising of the EEG signals affected by white noise (which is highly nonlinear, and is similar to the EEG); (iii) hardware limitations (distance and speed) of communication for portable and wireless devices (irrespective of Bluetooth and Wi-Fi) in real-time applications.

In the following, we explain the methods applied to identify the intentions of drivers based on brain signals.

III. IDENTIFICATION OF THE DRIVER's INTENTION

To detect and predict the driver's intention for the control of a BCV and a BCAV, the steps presented in Section II-C have to be followed. We will provide a brief review of each step in this section (supported by the information presented in Tables 1 to 2 in Appendix).

A. STEPS OF IDENTIFICATION ALGORITHMS

Conceptually, automatic identification algorithms are defined in offline and real-time processing, where the offline mode is used for training a classifier for the real-time processing; a list of classifiers that are used in identification problems and optimizers that can be used in training are shown in 1. In the offline processing, the steps listed in Section II-C have to be followed. The steps are well-known, and they are presented in brief as follows:

1. Preprocessing: proposed for removing unwanted signals that include segmentation, filtering, and normalization; all these techniques depend on the targeted patterns. For example, Alpha band (8–14 Hz) and Beta band (14–30 Hz) are usually used for movement and IM patterns.

2. Feature extraction: a good feature algorithm shows high distinction for a specific part of a signal against other parts of the signal. A short list of features for the BCV and BCAV applications are average, median, power, amplitude, variance, PSD, FFT, autoregressive, long-term correlation, cross-correlation, spectral amplitude, frequency-filtered signal (Alpha and Beta waves), Common Spatial Pattern (CSP), Independent Component Analysis (ICA), FastICA, wavelet, Detrended Fluctuation Analysis (DFA), chaotic algorithms, such as the largest Lyapunov exponent, and HbO and HbR (hemoglobin concentration) changes for the fNIRS.

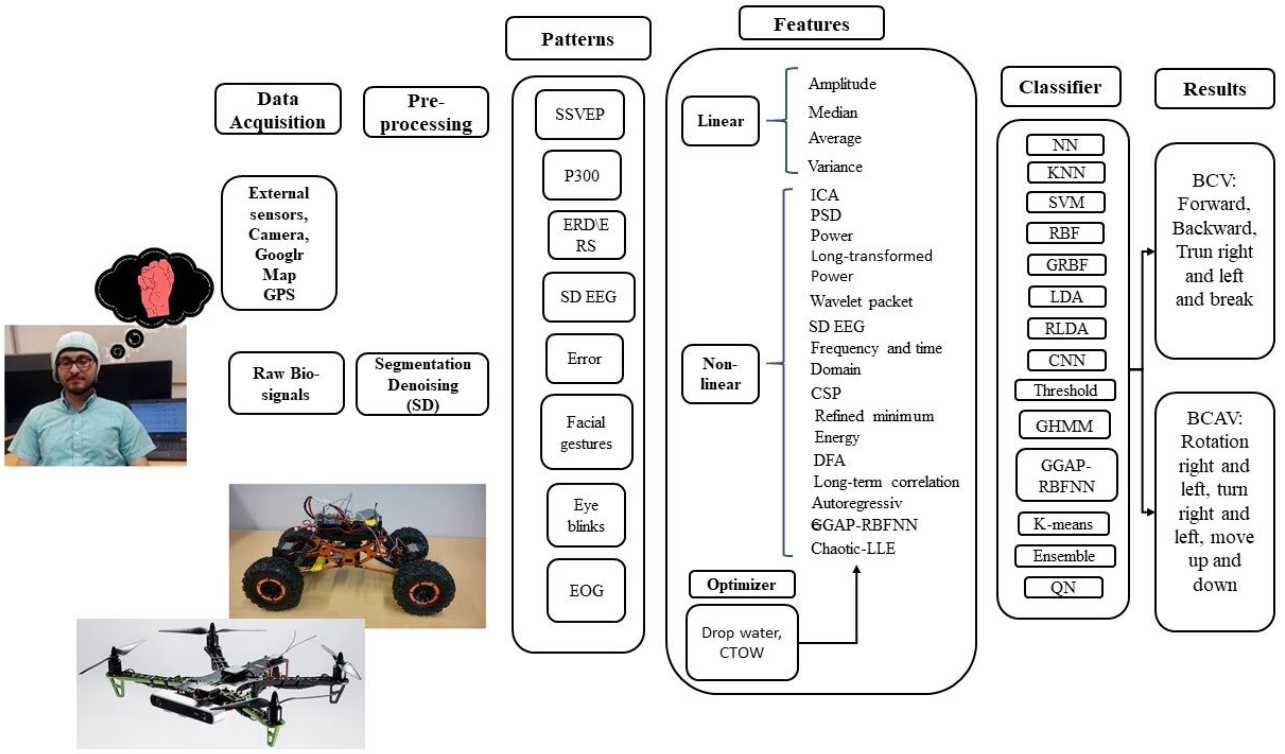

FIGURE 1. Algorithm's (features and classifiers) diagram for identifying the driver's intention for BCV and BCAV applications.

In some algorithms, the initial values of the features require optimization.

3. Feature selection: removing the irrelevant features by using feature selection algorithms. The irrelevant features are generated by noise. The feature selection algorithms used for BCV and BCAV applications are the Principal component Analysis (PCA) and the Linear Discriminant Analysis (LDA). The selected features are then fed into the classifiers for categorization.

4. Classifiers are decision-makers for the categorization of features. Classifiers are divided into supervised and unsupervised types. In the supervised algorithms, the labels of segmented signals for different classes are determined, whereas in unsupervised classifiers the labels are enigmatic. In the present review, supervised and unsupervised classifiers used for the BCV and BCAV applications are K-Nearest Neighbor (K-NN), LDA and Regularized LDA (RLDA), Neural Network (NN), a combination of RBFNN with GGAP-RBFNN, different combinations and modifications of (Soft Margin) Support Vector Machine (SMSVM) with (Generalized) Radial Basis Function (GRBF), threshold-based classifiers, such as Vector Phase Analysis (VPA), Queuing Network (QN), Logistic Regression (LR), Convolutional Neural Network (CNN), Ensemble Classifier (EC), Model Predictive Control (MPC), K-means, Gaussian Mixture Model (GMM), and Hidden Markov Model (HMM), which are discussed in Section IV, and whose details are summarized in Tables 1 to 2.

5. In order to increase the efficiency of features and classifiers, optimization algorithms are used. Optimization algorithms enable flexibility of the consistent parameters to overcome limitations of traditional features and classifiers. For example, Water Drop Optimization (WDO) and Chaotic Tug of War Optimization (CTWO) have been developed recently. Conceptually, the WDO is an evolutionary algorithm that has been developed based on the behavior of water in a river, the objective of which is to search for optimum values in functions. The idea of the algorithm is based on two characteristics of the water flow; 1) velocity and 2) number of soils conveyed by water. The advantage of this approach is high-speed convergence [23]. The second recently developed optimization algorithm is the CTWO, conceptually inspired by the rope pulling competition. The CTWO selects two teams as solution candidates for applying pulling forces (interaction between teams), and the magnitude of forces is relative to the quality of solutions. The algorithm has five steps; 1) initialization, 2) weight assignment, 3) competition, 4) new generation, and 5) termination. The advantage of the CTWO is its higher speed compared with the stochastic searches [3], [24].

6. Statistical analysis: in order to measure the efficiency of the classifiers, statistical measures, such as accuracy, sensitivity, and specificity are employed. In these algorithms, the computations are based on four parameters as follows: TP is the correct features that are correctly categorized as positive, TN is the false features (incorrect) that are correctly categorized as false, FP is the false features (incorrect) that are incorrectly categorized as positive, and FN is the correct features that are incorrectly categorized as false [25]–[27]. TP is an outcome where the model correctly predicts the

positive class, TN is an outcome where the model correctly predicts the negative class, FP is an outcome where the model incorrectly predicts the positive class, and FN is an outcome where the model incorrectly predicts the negative class. If the results obtained are satisfactory, the trained classifiers are then saved and used for real-time-experiments.

7. Real-time mode applications: In the reviewed papers, the following real-time BCV and BCAV applications were presented: a vehicle simulator, a graphical game, a real car in the real world, a mobile robot, a quadcopter, a drone, a helicopter, and an aircraft. In the following section, we describe studies on the control of BCV and BCAV applications in detail.

IV. STUDIES ON BCV AND BCAV

In order to control a vehicle by using bio-signals, different simulators and algorithms have been used as illustrated in Tables 1 and 2. Studies published on BCV and BCAV topics are related to detection of the driver's intentions to control a vehicle for navigation, changing the lane, steering control, [28], [29], the EBC [30], [31], and the OAC [22], [32]. The studies discussed here are divided into two parts; BCV and BCAV studies, which are organized into successful initial ideas (exploring patterns and how to generate patterns by using appropriate tasks), mathematical developments, and improvements to the current situation step by step. Some studies report accuracy results based on individual subjects; considering such studies, we have computed the average values of accuracies and report them in Tables 1 to 2.

A. TECHNIQUES EMPLOYED FOR BCV APPLICATIONS AND THEIR EFFICIENCIES

In the initial generation of key series studies, Haufe *et al.* [33] implemented an EBC system for BCV applications by using EEG and EMG signals in a graphical racing car task in the real-time mode. In the algorithm, the areas under the ERP patterns relative to the emergency brakes were computed and categorized using the RLDA classifier, and the efficiency was considered by accuracy and response time (reaction) parameters. The cons of the method are the low number of features, the limited ERP patterns for feature extraction, and the use of the linear classification RLDA. Therefore, different types and a larger number of ERPs for training of a nonlinear classifier for such a complicated signal (EEG) are highly recommended. It is noted that the ERPs vary over time in various situations.

In the study by Kim *et al.* [35], the objective was to overcome the limitations of previous studies by increasing the number of states for identification (soft and sharp braking) based on the driver's intentions. Each state has different task scenarios; soft braking refers to normal driving conditions, and sharp braking to a scenario with an obstacle on the road. In order to overcome the disadvantages mentioned earlier, features were extracted from three different patterns, such as RPs (time interval from 300 ms before the stimulation to 600 ms after the stimulation), the IM (ERD/ERS obtained by filtering EEG data between 5 and 35 Hz) and the ERP (obtained by Hilbert transformation). The results showed a higher accuracy to "...compared to the previous study in [33]. In addition, the authors reported that the area of the cortex which produce the ERP patterns relative to the emergency cases were determined. The limitation in the study of [35] was the low rate of robustness and the use of the binary RLDA classifier for categorizing more than two classes. The RLDA principle is based on the LDA algorithm, which is a linear classifier designed for binary identification. The LDA maximizes between-group scattering over within-group scattering. In other words, the algorithm searches for the projections by optimizing the feature space coordination, which reduces the inter-class variance whilst increases the distance between classes. By regularizing the LDA (RLDA), scattering of the inter-class features is regularized and enables a nonsingular matrix, which has the capability of employing a large number of features for the classification. The main limitations of the RLDA are the linearity of the algorithm and confinement to two state identifications [32], [36]–[38].

To solve the low robustness in the real-time experiment, Haufe *et al.* [39] extracted new features from the auditory signals in a vehicle-following graphical task for training of a RLDA classifier. The new trained algorithm was tested for the EBC in a real-world traffic case. The results did not report the accuracy and robustness of the algorithm. Overall, the presented series of studies aimed to extend the results by using patterns from EEG, EMG, and auditory signals. The significant advantages are variations of ERP patterns generated in different situations by using scenario tasks. The main drawback of the studies is that a larger number of subjects was not employed when using different classifiers.

External sensors, such as velocity, acceleration, wheel, and brake pedal angle sensors, and camera instruments, have been used to increase the accuracy of the method. Gohring *et al.* [21] employed a set of 16 external sensors with a camera for semiautomatic vehicle navigation on the road. To control steering and braking, ERD/ERS patterns from the EEG signal were extracted regarding the OAC and normal driving scenarios. The camera and external sensors used in the study helped significantly in decreasing the Evoke Potential (EP) detection error rates. The algorithm was then applied to a real vehicle, resulting in somewhat improved results. However, the reliability can still be considered insufficient because of the use of a low number of subjects and a threshold classifier, which is a known problem for single-trial algorithms. Even though a threshold classifier was used, the obtained accuracy is high enough.

The second generation of continuous studies aimed to overcome the defects of the previous studies by designing different tasks for generating new EEG patterns and developing mathematical algorithms for signal denoising, feature extraction, and selection. Bi *et al.* [34] designed a Head-Up Display (HUD) task and extracted SSVEP patterns to control a vehicle simulator. In the experiment, the first step was to identify the Alpha waves by using the LDA classifier to

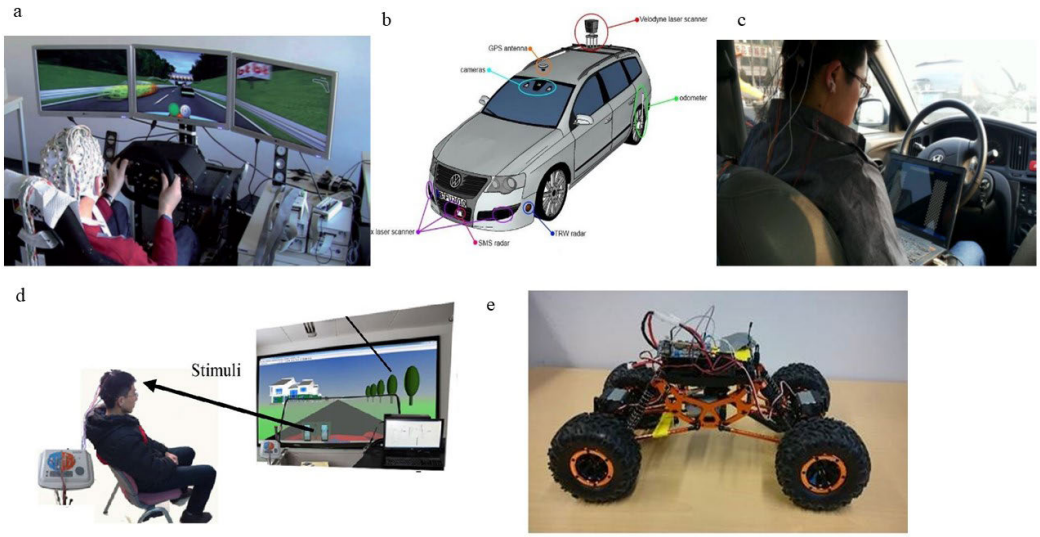

FIGURE 2. Different BCV applications: a) vehicle simulator [33], b) vehicle with different external sensors and a camera [21], c) real vehicle [22], d) video game vehicle [34], and e) mobile vehicle controlled by the EEG [29].

turn the vehicle on and off. Next, vehicle navigation (turn right, left, and move forward) based on the SVM classifier was implemented for the OAC. The results for the OAC and turning the vehicle on and off in the real-time mode were promising, but the results for the navigation in three directions showed high variation in accuracy. Limitations of the study were the small number of participants, the use of the SVM binary classifier for more than two classes, and neglecting the response time. Because of the constraints, the recommended speed for the algorithm was 30–40 km/h. In a subsequent work, Bi *et al.* [40] used an alternative pattern, viz. the P300 pattern for selecting the driver's intended destination for the same experiment as in [34]; the obtained results showed a higher accuracy with double the number of participants.

In the next subsequent study, Fan *et al.* [41] combined the SSVEP pattern and alpha EEG waves with the previous methods to control the vehicle simulator for the following commands: start, stop, stay on the lane, the OAC, and curve control. In the algorithm, the PSD features were extracted and categorized by the binary LDA algorithm, which has the same above-mentioned limitations. After this, Bi *et al.* [42] proposed a mathematical model for controlling the BCV steering in the same application [34] and [40]. The model was designed based on the QN algorithm for predicting the driver's intentions to navigate the vehicle in order to move forward and turn left and right. The QN was fed by the SSVEP patterns, velocity, acceleration, road information, and vehicle position in the road features to control the steering of a vehicle. The performance improved in comparison with the previous attempts, but compared with the other studies, the response time and robustness of the model were not reliable. The hallmark of the study is the use of an effective method for analytic equation solving, namely QN. The idea of the QN is to construct different models for predicting the waiting time in queues. For this purpose, the QN is constructed of three modules, known as preview, predict, and control modules. The input of the preview module is the path to determine the desired vehicle position, and the input of the predictive module is the road information and the vehicle state input provided by external sensors to determine the predictive position. The input of the control module is the subtraction of the preview from the predictive module to compute the error for the steering command computations. Therefore, the QN model is well constructed based on informative external features [42], but the algorithm would require more subjects to achieve a precise model. On the other hand, the EEG patterns vary considerably over time and in different situations, and thus, the PSD is not an adequate feature to predict the driver's intentions.

In a subsequent work, Bi *et al.* [22] limited the application to emergency brakes only. In the experiment, a set of above-mentioned and new external sensors (Table 1) were embedded into the system to analyze the conditions of the environment, resulting in a significantly higher accuracy and faster response in comparison with previous experiments [34], [40], [42]. The reason for the better result is the use of more sensors that provide more features, definition of only two states in the task, the use of the CSP algorithm, which is a powerful feature tool for binary states, and the use of the binary RLDA classifier. In total, the number of features increased and the number of classes decreased, which led to higher accuracy with less variation. The major concept of the CSP is to increase the feature space dimensions to maximize differences in variance between two classes, because the scattered features are divided into two categories; the reader is referred to more details in [37]. The SVM classifier made decisions based on features that are located at the margin of the two categories, namely the support vectors with a linear/nonlinear kernel. The main drawbacks were the

principle of the CSP algorithm, which is based on binary classifications. The idea of employing road data, as a future world-wide road map, is still open; to expand the method presented by Bi *et al.*, the road model has to be connected to a database, such as google maps, to obtain road information and weather forecasts with high-speed connection. Regarding the considerations of the study, the next telecommunication generations have the potential of solving the distance and speed constraints.

The same team, Lu and Bi [43] designed a controlling method to increase the safety of the user during longitudinal brain-control driving. The proposed method maintains the rear-end safety of the BCV while the user concentrating on the brain-controlling of the vehicle. In the algorithm, three models are defined as follows: 1- Longitudinal brain-control driving model for the driver decision behavior and brain-control operation behavior, 2- Vehicle longitudinal model for dynamic models of the host and preceding vehicles, and 3- Driver's behavior model for predicting the driver's decision. In the algorithm, predicting the driver's decision found from the SSVEP pattern at 12 Hz and 15 Hz, that features computed and feed into the SVM classifier. In this method, the safety is measured based on two measurements of minimum safe distance and a minimum time to collision. The obtained accuracy results were significant consequently the safety of the system were considered and achieved noticeable results.

Later on, the same team continued [44] and developed a controller named as robust sliding-mode nonlinear predictive for control of a mobile robot based on the EEG and HUD. Authors used the same HUD-based SSVEP as in their previous study [34] to increase the efficiency of the results in [43]. In the controlling algorithm, a cascading predictive controller which is for identifying the human intention is combined by a smooth sliding-mode controller which is designed for robust velocity tracking. In the algorithm, three classes were identified (forward, turn right and left) using the SVM (one vs others) algorithm. The results showed significant enhanced performance, higher safety, and robustness for control of a mobile vehicle. The safety has two points of view in the study, which are the distance safety of the vehicle during driving by use of a laser sensor and tracking the user attention during the task based on the SSVEP patterns at 12 Hz to 15 Hz. The obtained accuracy results showed significant improvement in comparison with their previous study [43]. It would be interesting if the researchers would use the Deep learning algorithm, which has potential of multi-class identification, even though the Deep Learning algorithm requires large number of input values for training. It might be covered using the large number of sensors. The disadvantage of the SSVEP-based methods is staring at the blinking lights for a long time for control a vehicle is not convenient.

The same team in a series studies, the aim was to increase the SNR and accuracy rate by combining classifiers. Lu and Bi [8] designed an algorithm based on the longitude control system to control the speed of a simulated vehicle. In the algorithm, the CSP was employed for augmenting the EEG signal SNR, and then, PSD features were extracted from the SSVEP patterns and classified using the traditional SVM classifier with the traditional RBF kernel. The accuracy of the results has high variations (low robustness) for individual subjects. Later, Lu and Bi [28] amended the previous study for longitude and lateral control. The idea was to extend the two classes to three classes with the same identification classifier, namely changing lane, selecting path, and following. Also in this case, the accuracy results showed the same high variation for the subjects. The studies had several drawbacks, as discussed above.

Later, the same team developed a control model including an optimization approach called MPC was by Lu *et al.* [45], [46] to increase the identification performance of the driver's intentions. The MPC was designed based on penalty values, which are obtained with a cost function for safety criterion parameters. The MPC model was a combination of two virtual scenarios; control of the road-keeping test and the OAC. The performance still has high variations. The novelty of the study was the use of the MPC method, which is an algorithm for controlling a process while satisfying the equation criterion. The remarkable advantages of the MPC are its flexibility and open formula for linear, nonlinear, and multi variable equations without a need to change the MPC control algorithm. One main disadvantage of the study is the use of traditional features and classifiers with low efficiencies, such as SVM and RBF. In the recent studies of the same team, Fei *et al.* [47] used a semi-supervised method based on adaptive algorithm for control of a vehicle. The adaptive method initialized the input values using a small labeled feature for a training set. Then, the initial values adjust automatically during updating with unlabeled new coming selected inputs. The study employed EEG patterns related to nine-character flashes for the users and extracting Mutual Information Maximization (MIM) features. The key points of the algorithm was employing a semi-supervised mutual information maximization (semi-MIM) feature selection algorithm that classified by Transductive Support Vector Machine (TSVM) classifier. The cons of the study were employing two subjects for the research, which is difficult to figure out how much the method is effective and small number of features.

In a set of different studies, various ideas based on combinations of sensors and traditional classifiers were implemented to increase the accuracies with higher reliability. Stawiki *et al.* [7] developed the control of a mobile vehicle by using a graphical user interface and a live camera feedback system based on the SSVEP patterns. The novelty of the algorithm was the adoption of a computational approach to remove noise and increase the amplitude of the SSVEP patterns before feature extraction, namely the refined minimum energy algorithm, which significantly affected the results.

Later, Hernandez *et al.* [30] designed an identifier for a vehicle brake system for considering different driving situations based on different scenarios. The preprocessed

EEG signals were the time-domain features, which were categorized by the SVM and CNN classifiers. The obtained response times for braking in the emergency cases (high speed) were insignificant.

In another recent study, Nguyen and Chung [48] developed a method for identifying the driver's intentions for the EBC in a vehicle. The algorithm consists of the EEG band power, auto-regressive model features, and an NN classifier. The results showed high accuracy and a significant improvement in the response time. The results have the potential for improvement if some of the features and classifiers are optimized. In general, the lack of subjects and nonoptimized algorithms is obvious, and moreover, improving the results by using simple models, such as auto-regressive, would require more considerations.

Recently, Dindorf and Wos [49] a system for the EBC using the EMG signals, named as dual brake pedals. Also, authors designed a new application using a Pneumatic Actuator as a secondary foot brake pedal to increase the safety by increasing stopping power. In the method, muscular signals from the partcipant's face and eyelids, clenching of jaws, and pressing tongue on the palate were measured for controlling the brake pedal. In the algorithm, feature extracted from a low pass filter (15 Hz) signal and spectral analysis. The evaluation of the results was based on the brake pedal deflection that computes by the lowess method filter and lase sensor. In the presented method, the reaction response for the signal processing was 0.02-0.05 s and the reaction time for the pneumatic system was 0.23 s, the best obtained response time was 0.24 s. The cons of the method are due to the use of pneumatic system instead of electrical break the reaction time is high and expose the diver in dangerous situation. Also, statistical analysis such as accuracy, sensitivity and specificity did not evaluated. In the next study, Dindorf *et al.* [50] used the EEG, EMG and eye movement signals to increase the efficiency and safety of the user. In the study, it is claimed that the user safety is improved by decreasing the reaction time of the system in an EBC task.

In another study, supervised and unsupervised classifiers were combined to raise the accuracy rate. Zhao *et al.* [51], designed models for the driver's intention for braking. The model was a combination of the GHMM/GGAP with RBFNN (GHMM/GGAP-RBFNN). The algorithm was designed for identifying slight and normal braking states and then tested in a real vehicle. The results obtained were significantly improved compared with their previous work [52], but the time response was not taken into consideration. The novelty of the method is the optimization of the network connections in an NN by using GHMM/GGAP approaches, where the GHMM is a combination of the unsupervised GMM and HMM algorithms. Conceptually, the GMM assumes that each class has a Gaussian distribution, and the feature space consists of a mixture of a number of Gaussian classes, which follows the rule of mixing finite Gaussian distributions, each Gaussian having a specific center and width. In the study, some GHMM parameters were computed using the HMM clustering algorithm. In short, the HMM is an extension of the Markov Model (MM), the principle of which is based on the Markov Chain (MC). Conceptually, the HMM is based on observable patterns that are relative to unobservable interior factors, namely patterns and states, respectively. The algorithm has two random processes for the layers, called hidden and visible processes for the hidden states and observable patterns, respectively. The hidden states compute the MC and the probability distribution of the patterns relative to the states. The features are then categorized based on the probability computations [53]. Next, the GHMM is then employed to compute the parameters in the GGAP algorithm that links the aim of desired accuracy of the RBFNN with the importance measurements of the closest added new neuron, which is computed using the average content of the specific neurons. In general, the RBFNN is a supervised classifier, based on the feed forward NN with the traditional RBF activation function. The RBFNN contains input, hidden, and output layers, in which connections between the RBF activation functions have been pruned using the GHMM/GGAP-RBFNN method. In such a combination of complex and unsupervised methods, disadvantages are the delay for real-time processing, a high error rate, and low robustness. One easier approach to improve the results is to optimize the sensitive initial values in the features and classifiers.

Later on, Liu *et al.* [54] employed lidar simultaneous localization/mapping technique for navigating. In the algorithm, the SSVEP patterns used for control of a vehicle. The SSVEP patterns where generated using four different frequencies and the patterns were recorded by eight EEG sensors. Then, features classified by Filter Bank Canonical Correlation Analysis (FBCCA) that improved the CCA method results in previous their study [55]. Because the correlation is the main decision maker, no training set procedure is required. The achieved results for such a high speed processing method showed significant improvements.

In a recent continuing complementary study, optimization approaches included identification algorithms for adjusting features such as CSP and chaotic features and tuning classifiers such as traditional SVM and Radial Basis Function (RBF) for the BCV applications. In our previous experiment [37], [56], a method for controlling a mobile vehicle was implemented for moving forward and braking states, and the same method was applied to a prosthetic hand. In the procedure, Filter Bank CSP (FBCSP) features were optimized using the Discrimination Sensitive Learning Vector Quantization (DSLVQ) training algorithm, and then, different combinations of classifiers were employed. In the study, 14 different classifiers were implemented: KNN, NN, and different combinations of the traditional SVM, generalized SVM called Soft Margin SVM (SMSV), traditional RBF, and Generalized RBF (GRBF). The results showed that the DSLVQ optimization coefficients changed the CSP features, and the SMSVM classifier using the generalized RBF (GRBF) kernel, namely SMSVM-GRBF, yielded the best results. The advantages are 1) optimizing the features by the DSLVQ iterative learning

method. In the case of a low number of subjects, specifically in single-trial experiments, the DSLVQ optimizes features, which effectively overcomes the defects related to the lack of subjects. 2) By implementing the GRBF kernel in the SVM, the parameterized Gaussian function adds flexibility to alter the Gaussian shape for covering the distribution of the scattered features in each class, which leads to reliable accuracies with low variations [25], [27]. 3) Adding flexibility to the traditional SVM by deploying free parameters in the cost function and regularization algorithms. The drawbacks of [37] was the use of the CSP and the SVM, which are, in principle, designed for two classes as mentioned above, and therefore, the extended CSP approaches for multi-classes significantly increase the error rates.

Later on, we employed nonlinear features for identifying the ERD/ERS patterns for braking and moving a remote vehicle forward [5], [6], [29]. In the algorithm, the ERD/ERS patterns of individual subjects were employed as a mother wavelet in the wavelet packet. Then, the Detrended Fluctuation Analysis (DFA) method was used for computing a new time series based on the wavelet components. The long-term correlation features were then extracted and classified by the SMSVM-GRBF [37]. The advantage of this method is the use of an individual's ERD patterns to compute wavelet components, the results of which were shown to be well optimized. The drawbacks of this method are the delay in the real-time experiment, which was about 1.5 s because of the wavelet. Furthermore, the limitation of the 12 m distance for controlling the vehicle was a further limitation that was due to the XBEE bluetooth chipset, yet it can be solved by using Internet of Things (IoT) and 5G technologies.

In the next step, the objective of our team [3], [26] was to improve a nonlinear chaotic feature extraction method for the same application based on the ERD/ERS patterns. In the algorithm, the Largest Lyapunov Exponent (LLE) was computed, and then, the initial values were optimized by using the WDO [57] and CTWO [3] optimization methods. The results were improved in comparison with the normal LLE only in the offline mode, but the algorithm was not useful in the real-time mode because of the LLE limitations. The LLE is well optimized only for a signal length of more than 1.5 s, which causes delay in real-time systems. The advantage of this method is the use of evolutionary and chaotic optimization methods, known as the WDO and the CTWO. The drawbacks of the evolutionary optimization algorithms are that the proposed optimized answers are not always the best values, and they are highly dependent on where the search engine starts for seeking the optimized values, and further, the onset points are selected randomly as explained in III-A.

A close complementary series of study is related to the identification of the driver's emotions, where the emotions during driving are termed as nervous and relaxed. Zhang *et al.* [58] designed a real-time algorithm based on error-related potentials to control a simulator and a real vehicle. The LDA classifier was then applied to control speed, lane change, and dynamics of a vehicle. The results could not provide remarkable improvements in comparison with the previous studies. The drawbacks of the studies are similar to the above-mentioned methods; in short, a low number of subjects and features, and using a very basic binary linear classifier to identify more than two states. Therefore, Yang *et al.* [59] limited the previous study [58] by designing a binary classifier for predicting only two states of the driver's emotions, namely, aggressive and unaggressive. In addition, a larger number of features, viz. amplitude, long-transformed power, and PSD from different frequency bands were computed. The final model was a driver assistant for lateral (changing lane) and longitudinal control (speed acceleration). The novelty of the method was the design of two identification layers, which consist of two supervised (SVM, KNN-based on voting) and one nonsupervised learning (K-means) classifiers. The K-means algorithm concept solves a minimizing within-cluster variance enigma to reach a K number of clusters. In this context, we should bear in mind that the unsupervised methods usually have higher error rates, yet they are effective when integrated with supervised methods. The limitations applied to the number of classes and the use of a binary classifier improved the results, even though feature selection and optimization for classifiers was not used. The tuned classifier means adjusting the initial values and correcting error rate coefficients in the classifiers to minimize the error rates. The tuned coefficients result in effective selection of support vectors in the SVM, which play a critical role in fixing the margin and the decision hyperplane. Regarding the presented studies, the traditional features and classifiers required optimization that was addressed in detail [37].

Next, Zhuang *et al.* [31] implemented an EEG-based algorithm with real-time visual feedback to control a simulated vehicle for controlling a BCV in three states of right and left steering and acceleration for the OAC task. Zhuang *et al.* employed a combination of wavelet and Canonical Correlation Analysis (CCA) to reveal the ERD/ERS patterns. The PSD features were then identified by using ensemble, SVM, and CNN classifiers. The CNN is a three-layer classifier in the DBL, namely convolution and pooling layers. The constructed CNN has an ability of having several convolution and pooling layers that the number of layers requires to be adjusted. The convolution layer is employed to produce features from the input data. The pooling layer is then employed for dimension reduction of the convolution layer and the NN for classification. The CNN approach is highly effective when a large number of features are available. Finally, the EC reaches the best result, which is a combination of several learning algorithms in a classifier. The EC is known as a generalized approach to increase the efficiency of any classifiers in comparison with individual classifiers, such as boosting and bagging methods. Boosting is a popular method in the EC for reducing bias to obtain a strong dependence in the data [31]. The drawbacks of the study is the use of a time-consuming algorithm, called wavelet, which causes delay in real-time systems.

The second interesting type of vehicle is aerial vehicles. Many attempts have been made to control the BCAV by using bio-signals. In the next section, the methods used to control a BCAV are considered in detail.

B. TECHNIQUES EMPLOYED FOR BCAV APPLICATIONS AND THEIR EFFICIENCIES

In the present review, examples of the second type of vehicle, aerial vehicles, are illustrated in Fig. 3, including drones, quadcopters, helicopters, and airplanes. A review of aerial vehicles controlled by BCI [60] was published in 2018, which presented studies published before the year 2015. The publications between years 2013 and 2015 are mostly conference papers focusing on categorization of types of aerial vehicle, applications, and control methods in general contexts. Here, we present a detailed complementary methodological review based on effective bio-signal processing studies over the past ten years.

Drone technology is a commercialized application that many industries and organizations have been deployed to increase their productivity and efficiency. The combination of unmanned aerial vehicles and BCI is a new idea. The advantages of using drones are significant; e.g., low-cost production, transport and maintenance, readiness to fly quickly, exploitability in perilous situation, use of clean energy, and suitability for demanding applications, such as spacecraft [64]. There are many categories of aerial vehicles for different applications, such as health care and military use. In the present survey, the focus is on the review of bio-signal processing techniques for the control of BCAV applications in the nonmilitary use. Considering other types of aerial unmanned vehicles, structures and electronics, the reader is referred to [64]–[66].

Recently, hybrid methods have been employed to control aerial vehicles, such as EEG, (f)MRI, and (f)NIRS measurements. The fNIRS and fMRI methods have the limitation of real-time mode usage, but they have a high resolution. On the other hand, the EEG can be used in the real-time mode, but it does not have as high a resolution as the fNIRS and fMRI instruments. Therefore, some studies combine the advantages of the both techniques simultaneously and introduce hybrid methods, such as the EEG with the fNIRS [67], [68], the EEG with the fMRI, and the EEG with the eye tracker [69]. In the EEG-based aerial control algorithms, the following patterns employed for feature extraction are the ERD/ERS, ERPs, SSVEP, eye movements, and blinking. The features computed for the above-mentioned patterns are cross-correlation, LR, mean, peaks, and PSD, which are classified with different classifiers, such as the SVM [67], [70] and the LDA [68].

In general, the control algorithms of the BCV applications are well explored and could be employed in the BCAV applications. The difference between the control of the BCV and BCAV applications is four navigation commands, such as take-off (up for drones), landing (down for drones), rotations for drones (different from turning), and keeping balance, which are not considered yet. The preliminary navigation commands employed for the fixed wings and helicopter control the four main directions after manually taking off, which is the most similar navigation to the BCV control applications.

In a continuous series study, Royer *et al.* [61] aimed to establish a control for a graphical helicopter in four main directions using the ERD /ERS patterns. In the algorithm, the extracted features were cross-correlation and difference of the auto-regressive spectral amplitude between the right and left hemispheres. Three weaknesses of the algorithm were a delay of 2.1 s in reaction time, the use of a linear classifier for four states, and low precision.

In another study, Akce *et al.* [62] used the ERD /ERS patterns to control a fixed-wing aerial vehicle. In the experiment, the fixed wings were controlled based on selecting a trajectory of a flying path through a binary classifier. The algorithm has the same limitations as in [61]. As an open study, we suggest that in the case of specifying flying path methods, it is possible to use methods similar to the inverse kinematics to optimize the feature values in the control system to let the fixed wings reach the end point. Doud *et al.* [71] improved the results of Royer *et al.* [61] by using a control of a virtual helicopter for six directions based on the time-frequency analysis and PSD features.

Finally, the helicopter accuracy results were improved by Lafleur *et al.* [63] for the control in six directions based on the IM patters (SSVEP, ERD/ERS). The limitations of BCAV methods are the same as the BCV methods, which are considered in IV-A.

In a continuous hybrid series study, Kim *et al.* [69] developed the control of a quadcopter in eight directions based on eye gaze in nine points by using an eye tracker and EEG signals. The selected features were pupils of eyes from the camera, power of the EEG, and EOG paradigms. The main drawbacks of the study were the use of the traditional SVM classifier with a linear kernel and a low number of features and subjects. A different approach was provided by Shi *et al.* [72], who controlled a hex-copter with a live feedback camera for the OAC application. The application was controlled by using the ERD/ERS patterns. In the algorithm, cross-correlation features and LR classification were used. The LR is a variable-dependent binary linear supervised classifier, which is based on a logistic function (S-shaped function) in a statistical model. The objective of the LR model is to model the probability of the features related to individual classes, such as imagination of right- and left-hand movements. In other words, the function of the LR is to find a linear decision boundary between classes by using the parameters that are assigned to the features. The computations are based on the relation between the dependent binary variables of the classes and the maximum likelihood estimation. The weights are then adjusted and applied to the features for classification. The idea was developed further by Coenen [16], who limited the number of classes and used different techniques of response to mental task patterns accuracy to control a drone in two directions. The signal was recorded

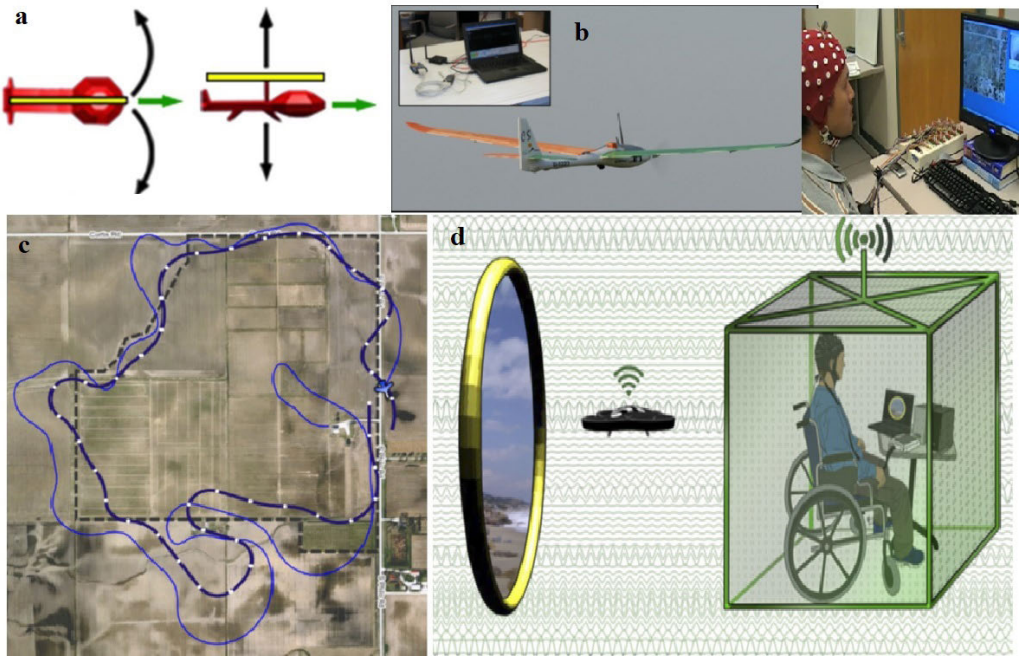

FIGURE 3. Some applications used for BCAV: a) virtual helicopter [61], b) fixed wings [62], c) control based on following a selected path [21], and d) quadcopter [63].

in an auditory imagination and spatial navigation mental task. The different patterns generated and the low number of states were the key improvements to the results. Next, the objective of Kosmyna *et al.* [73], [74] was to control a quadcopter in three directions by using a hybrid EEG and EMG bio-signals. In the task, left- and right-hand IM and foot tapping were employed to generate the patterns to control turning right and left and moving down, respectively. In the algorithm, the IM patterns with the facial patterns were extracted from the EEG and EMG signals, respectively. The features were then identified by using the KNN algorithm and adaptive recurrent NN classifiers. In the results, despite having a low variation, the reported accuracy was relatively low, which leaves room for improvements.

In a study, Duarte *et al.* [75] implemented an algorithm based on the CSP features and the LDA classifier for control of a drone in two directions. The aim of authors was implementing a low cost method for a brain-controlled drone using an open source software. The algorithm has limitations of number of subjects, classes and features. Study has potential of using other frequencies and EEG patterns and optimized methods. Then, Vishwanath *et al.* [76] implement an algorithm to control a quadcopter. In the algorithm, the CSP algorithm was used for computing features and then classified using a nonlinear SVM-based and LDA classifier. The LDA obtained the best average results. The drawback of the study was not mentioned what type of movements used for controlling and the results of a two-class classifier is compared with a four-class classifier.

Some studies have used the same BCV experimental tasks to produce different patterns; for instance, Kryger *et al.* [77] controlled an aircraft simulator in six directions by using the EEG. In the experiment there was only one subject participating in the study, and the authors did not report the mathematical methods applied in the study. Regarding the achievements of different patterns the SSVEP become a key point for brain-controlled navigation. For example, Wang *et al.* [55] proposed a method based on four different flickering LEDs for generating SSVEP patterns for the control of a quadcopter in four directions. The authors employed a Head-Mounted Device (HMD) in a virtual task. In order to identify the SSVEP patterns, the CCA with a threshold classifier was used. The reported accuracy for one subject was high, and it is suggested that only the threshold classifier would require critical considerations.

In another study, Chiuzbaian *et al.* [78] used the SSVEP features for a multi-class system to navigate a drone. In the algorithm, frequency features used for identifying four classes. The classifier was a threshold-based classifier that the edges were computed based on the maximum and minimum frequencies for each task. The simple threshold classifier reaches to a significant TP results. The drawback of the study was accuracy, t-test statistical analysis were not computed and results were not compared with other studies. In the next study, Duan *et al.* [79] combined the previous studies for navigating a quadcopter. In the algorithm, raw EEG signal, SSVEP and eye blinking patterns form EEG were employed for features computations. The computed features were as follows; 1- Complete information common spatial pattern (CI-CSP) features extracted from the raw EEG signal for turning left and right actions; 2- CCA features extracted from the ERD/ERS SSVEP patterns for takeoff and landing; and

3- Eye blinking features for switching between two flight modes of turning in part 1 and landing and/or take of in part 2. Significant results showed the efficiency of the CCA and SSVEP for controlling a quadcopter. The advantages of the study were employing the powerful features CSP and CCA. The results would be increased and be more stable if larger number of subjects were used.

An idea of combining the EEG and fNIRS signals in the real-time mode has been proposed. The first series study was performed by Lin and Jiang [80] to control a quadcopter in six directions. In the algorithm, EEG and EMG signals were recorded in a facial gesture task. The features were computed based on the EEG signals, and the numbers of features were then reduced by using the PCA feature selection. The achieved accuracies using this approach have not led to significant improvements with respect to the original work. Moreover, Khan *et al.* [81] recorded data based on the IM tasks for two directions. A combination of the ERD/ERS and SSVEP patterns was used for computing the PSD features. Oxygenated and deoxygenated hemoglobin features were extracted from the NIRS data. The results showed significant changes. After that, Jackson [82] developed further the idea of Khan *et al.* [81] to control a quadcopter in six directions by a Google glass with the EEG signals. In the experiment, a task based on head posture movement imagination was designed. Spectral features of the ERD/ERS and SSVEP were then computed as in [81] and selected by the PCA. The identification algorithm was also a combination of 14 external sensors for navigation. The accuracy results were not significant. The main downside of this study was the use of a traditional SVM classifier with the traditional RBF kernel for multiple-class identification. Furthermore, the presence of the PCA was not considered, because the PCA removes the effective feature space.

In the next step the same group, Khan *et al.* [83] used the EEG, EOG, and FNIRS data for extracting features in four directions and conducted tests in a real-time experiment. In the algorithm, left-hand IM and left- and right-eye movements were used to navigate the quadcopter with live video feedback. In addition, an OAC algorithm was developed by using the SSVEP patterns. This method has the constraint of using only three subjects and binary classes.

After this, Khan and Hong [68] focused on generating new EEG patterns based on different brain stimulators, such as mental arithmetic, mental counting, word formation, and mental rotation. The features were peak, skewness, mean, and power from the EEG and mean, peak, slope, peak, minimum, and skewness of the fNIRS signals. The results were improved by comparing them with the previous approaches reported in [81]. The number of features reduced the limitations of the study; nevertheless, different classifiers were not considered.

Next, Khan and Hong [68] enhanced the EEG-fNIRS method by exceeding the number of decoded commands to eight commands (clockwise and counterclockwise rotations added) for the control of a quadcopter. In the experiment, two LDAs were employed for classification. One LDA was used to classify the fNIRS features, and the others for the EEG features. The decision to divide data into two sections for the use of the LDA improved the identification results. However, the lack of using nonlinear and optimized classifiers for multi-classes is obvious.

In a subsequent work, [67], used only fNIRS signals to control a quadcopter for one state of moving forward. In the algorithm, mean, slope, peak, changes of HbO and HbR, and HbT and COE features were used and categorized by the traditional SVM, threshold circle, and vector phase analysis classifiers. A weakness of the study is the low number of subjects, unoptimized classifiers, and a delay of 2.3 s. Therefore, the same team, Zafar *et al.* [70], conducted another study for controlling the drone for three states of up, down, and moving forward. To this end, mental arithmetic and mental counting tasks were employed with the same algorithm as in [67]. Improved results were achieved compared with their previous study [67], but the limitations remained as before; there was a 2.3 s delay in the real-time system, which is inefficient. Recently, Kavichai *et al.* [84] were able to reduce the time delay in [68] by using the Shared Control Strategy (SCS) method. The SCS method employed environment information by using external sensors. Therefore, Kavichai *et al.* combined the fNIRS and EEG features with the following three measurements: eye movement, distance (measurement sensor), and Global Positioning System (GPS). Finally, four commands were controlled by the fNIRS signals, and four other commands by the EEG. The aim of the approach was the OAC and reducing the time response delay. Based on the studies, the topic is still open and has a high potential for improvements.

In recent studies, Chen *et al.* [85] combined the EEG and EOG signals to navigate a quadcopter. In the algorithm, three types of features were computed as follows: 1- CSP features from imaginary (ERD/ERS) patterns of right- and left hands; 2- First set of dual-tree complex wavelet transform (DTCWT) from the EOG and 3- Second set of EOG features which are eye blinks, Vertical EOG (VEOG), Horizontal (HEOG) and waveform features. The key point in computing the EOG features is first computing dual-tree complex wavelet transform (DTCWT) coefficients to obtain the maximum wavelet coefficients, area under the curve, amplitude, and velocity. The third types of features were computed by differential counting algorithm to identify the number of consecutive eye blinks. The proposed method reach significant accuracy rates for a limited number of subjects. To evaluate the accuracy and precision results larger number of subjects is needed. In the next recent study, Kim *et al.* [86] used imaginary tasks for controlling formations of swarm drones in four classes of Hovering, Splitting, Dispersing, and Aggregating, the details of definitions are available in the presented reference. In the algorithm, CSP features, power of Alpha waves for different frequencies were extracted and classified using the LDA, SVM, KNN, Decision Tree (DT), and ensemble methods. Results showed that the EEG in 8-13 Hz has the most

informative imaginary information. The advantage of the method was reach to significant accuracy results using the basic LDA classifier by use of low number of features and subjects.

Later on, Kogava and Kai *et al.* [87]–[89] developed a method for controlling a drone for amyotrophic lateral sclerosis patients in a three-step studies. In the approach, only microsaccades eye movements used for operating the drone using an eye tracker. The study focus on designing a the experimental setup and task. In the experiment, six subjects attended to take control of a drone by performing a task on a monitor for five degree of freedom, the data was transferred by internet. The AI algorithm for identifying the commands and employed statistical analysis such as accuracy and precision is absent, the study focused on the experimental setup details. Next, Kapgate [90] utilized SSVEP and P300 patterns simultaneously to control a quadcopter in the real world. In the task four main directions navigated using the SSVEP and P300 features. In the algorithm, the SSVEP pattern were extracted from the Alpha (8–13 Hz) and Beta (14–26 Hz) frequency bands and then the PSD features were computed. At the same time, the p300 waves extracted from 0.1-12 Hz frequency band. The signals were discriminated using the CSP algorithm and then classified by the LDA classifier. The results were well-analyzed statically and significant results were obtained. The limitations of the study could be named as variation of accuracies for individual subjects, more number of classes are needed for complete control of a quadcopter. Also, more number of features for higher accuracies is recommended.

There are differences in the control principles of the BCV and BCAV applications. The BCAVs have eight degrees of freedom for flight, but the BCVs are limited to four main directions. The main challenge in the BCAV is keeping balance whilst moving in any direction; none of the studies have considered this aspect. Therefore, more error rates to control BCAVs are generated, which requires more accurate features and classifiers. All in all, the advantages of the methods are designing new tasks for identifying patterns relative to the specified actions. Also, some of the employed algorithms achieved good accuracy results for finding imaginary movement patterns, but the variation of the subjects is still high which can be controlled for some levels using regularization methods. The challenging points for the BCV and BCAV applications are associated with finding nonvariant patterns, reducing response time, and optimizing features and classes. Multi-class identification for higher precision and robustness are still problematic and cause error rates for offline and real-time systems. The drawback of most of methods were using the traditional methods with no optimization and no creative ideas in the classifications step. Also, employing advantages of different methods in previous successful methods is seen in a few studies, which has high potential of future research. In summary, according to the presented studies and achievements, the DSLVQ, for instance, could be considered an efficient method for enriching the features (and similar algorithms for future research), and the best known classifiers for controlling the BCV and BCAV applications could be EC, DBL, and SMSVM with GRBF kernel classifiers.

V. FUTURE PERSPECTIVES

In the presented BCI studies, bio-signal patterns have been deployed to control BCV and BCAV applications. Detecting the driver's intention for emergency braking is a challenging task in the real world, where stress, fatigue, mental workload, different emotions, and environmental noise are present and vary individually. The second challenge in the BCV and BCAV applications, specifically related to emergency braking based on bio-signals, is the response time. The question is how much time is needed to prevent a collision at different speeds; this is a topic that requires further considerations. Furthermore, reducing the delay of time-consuming algorithms in real-time systems with high accuracy and robustness is yet another challenge, which has great potential for investigation. Despite the above-mentioned noise, identifying the emergency braking situation based on the EEG involves high risks. Emergency cases such as obstacle avoidance have certain limitations: 1) identifying an obstacle is different from predicting an obstacle, which is a difference between a real dangerous situation or something with a potential of danger; 2) environment has a highly negative influence on the results, which increases the risk rate.

The third critical issue is the limitation of distance for communication systems in the BCV and BCAV applications. The solution would be to integrate the BCV and BCAV with new technologies that are supported by 5G systems (e.g., [91]) that have great potential for a higher quality of communication with virtually no delay as in real-time processing. The high-speed communications enable the applications to load a high amount of data in cloud/edge servers to store and use them within strict time constraints. Moreover, it is more applicable to use road information through the Internet for different applications. The fourth critical limitation is the issue of the reliability of the application security [92], which is a crucial topic for future research. The security investigations have two aspects: 1) security of a system against hacker attacks; and 2) security of a system when a fault happens during the control of an application. Before using the BCV and BCAV applications in the real world, the security issues related to decision-making in fault situations have to be solved to avoid irreparable damages. The fifth critical issue is developing accurate systems for alerting the user when the user's concentration drops [93]. If a paralyzed patient want to use a BCI system as a carrier, the user should concentrate for a long period of time, for example eight hours. Therefore, an accurate alerting system is required to analyze the feeling of the user during work such as alpha waves monitoring, eye tracker and/or video processing to inform how is the user situation and how the user should proceed the work. The sixth future issue of the BCAV applications is the air traffic challenges [94]. The solution would be

TABLE 1. The reviewed studies over the past ten years.

Authors Year	Signal	Patterns	Features	Classifiers	Task and control commands	Average Accuracy	RT	Modes
Haufe et al. [33] 2011	EEG, EMG, Gas pedal	ERP	1) symmetric negative deflection in occipito-temporal area, 2) negativity at central scalp sites 3) positive deflection around electrode CPz and 4) area under the ERP curve	RLDA	behavioral response to EBC	83.00% passing collision	130 ms	OM, POM
Gohring et al. [21] 2013	EEG, 16 external sensors, camera	ERD/ERS	pre-processed EEG signal	Threshold	R, L, S, B for Path selection, braking, steering	90.00%	26% less than 2 s and 36% between 5–10 s	OM, SAM
Bi et al. [34] 2013	EEG	SSVEP, alpha waves, HUD	PSD	LDA, SVM	L, R, B, S for start, stop, stay in lane, OAC and curve control	SSVEP detection= 76.87% alpha wave detection = 93.53%	2 s to 3.5 s	RTM, OM
Bi et al. [40] 2013	EEG	P300	PSD	LDA, SVM	L, R, S for destination selection	93.60%±1.6	12 s	RTM, OM
Kim et al. [35] 2014	EEG, EMG	RP, ERD/ERS ERP (visual evoked potentials, p300)	RP features = 300 ms before stimulation to 600 ms after stimulation; ERD/ERS features = EEG between 5 Hz and 35 Hz; and ERP features = Hilbert transformation of data	RLDA	RFM, SIM, ES for sharp and soft braking intention	-	150 ms	OM
Haufe et al. [39] 2014	EEG, EMG	ERP	The same as [33]	RLDA	the same as [33]	-	RTM = 200 ms, RVM = 237 ms	RVM on a non-public test
Fan et al. [41] 2014	EEG	P300, SSVEP	EEG= 0-512 ms time interval after P300 onset	LDA	destination selection	OM = 99.07%±0.40, RVM = 98.93%	OM RT selection = 24.19 s±0.85 s, RVM RT = 25.95 s±1.04 s , no response time	OM, RTM, RTM
Zhang et al. [58] 2015	EEG, EOG	filtered error -related potential	PSD	LDA	L, R, S for controlling speed, lane change and dynamic of vehicle	OM = 69.80%±6.50 RVM = 68.20%±5.90	-	OM, RTM, RVM
Bi et al. [42] 2016	EEG, road information	SSVEP	Frequency-domain features	Extended queuing network developed four-class graphical user interface [7]	L, R, S for turning left, right and going forward	88.77%±13.5	500 ms for model processing, RT not mentioned	OM, RTM
Stawiki et al. [7] 2016	EEG	SSVEP	refined minimum energy [7]		L, R, S, B for turn left, right, forward and stop	93.03%	-	OM, SAM
Teng et al. [32] 2017	EEG	denoised EEG signals	CSP& PSD for different frequency bands	RLDA	S, B for EBC	94.00%	420 ms	OM, PO, RVM

L = Left, R = Right, S = Steering, B = Brake, BW = Backward, RFM = Right Foot Movement, SIM = Self-Initiated Movement, ES = External Stimulus, RTM = Real-time Mode, OM = Offline Mode, POM = Pseudo-real-time Mode, RT = Response Time, SAM = Semi-Autonomous Mode, RVM = Real-Vehicle Mode.

developing an air traffic system for control of drones how and where to move to prevent air crashes. Also, the UCAV systems required to be equipped with different systems in case of UCAV accident situations. By solving constraints and reaching the highest accuracy and reliability, potentially new jobs and technologies may be launched, some skilled disabled people may be able to return to their previous duties, various tasks in remote locations can be performed faster,

TABLE 1. ***(Continued.)*** **The reviewed studies over the past ten years.**

Authors Year	Signal	Patterns	Features	Classifiers	Task and control commands	Average Accuracy	RT	Modes
Wang et al. [95] 2017	EEG	denoised EEG signals	falling-off discrimination model	RLDA	S&B for EBC	99.63%	-	OM
Hernandez et al. [30] 2018	EEG & EMG	denoised EEG	time domain	SVM & CNN	Left leg movement for EBC and OAC	SVM = 71.10%, CNN = 71.80%	718±162 ms	OM & RTM
Bi et al. [22] 2018	EEG & external sensors	denoised EEG signals	CSP	RLDA	S&B for EBC	94.89%	540 ms	OM, PO & RVM
Yang et al. [59] 2018	EEG	denoised EEG	FFT&ICA	long-transformed PSD different bands& power amplitude	SVM, KNN and K-means with adaptive synthetic sample	S&B for aggressive and unaggressive behavior	69.50%	OM
Lu et al. [8] 2018	EEG	SSVEP	PSD	SVM with RBF kernel	S&B for lane changing, path-selection, and car-following	no average, accuracy variation 49.70% to 100%	-	OM & RTM
Zhuang et al. [31] 2019	EEG	ERD/ERS	CSP	SVM,CNN& ensemble model	L, R, S, B for OAV	CNN = 87.17%, SVM = 83.25%, ensemble model= 91.75%	-	OM & RTM
Hekmatmanesh et al. [5], [29] 2019	EEG	ERD/ERS	Wavelet-DFA, long -term correlation	SMSVM with GRBF kernel	S & B for moving forward and braking	85.33%	-	OM
Hekmatmanesh et al. [3] 2019	EEG	ERD/ERS	optimized LLE using CTWO	SSVM with the GRBF kernel	S&B for moving forward and brake	68.25%	-	OM
Lu et al. [28] 2019	EEG	SSVEP	optimized CSP, PSD	SVM with RBF kernel(one against others)	L, R, S, B for changing lane, selecting path and following cars	average accuracy not mentioned, accuracy variation 44.20% to 100%	-	OM, RTM
Lu et al. [45] 2019	EEG	SSVEP	frequency-domain	SVM with MPC	R,L,S for road-keeping test and obstacle avoidance	no average values, variation from 85.95% to 99.95% task success <50 ms%–100 ms%	-	OM, RTM
Nguyen et al. [48] 2019	EEG	preprocessed EEG	Five PSD frequency bands	NN	S, B, for EBC	91.00%	600 ms	OM, RTM
Zao et al. [51] 2019	signals of brake pedal stage	-	power& autoregressive	hybrid model of GHMM and GGAP-RBFNN	slight, normal and EBC	slight braking = 95.57%, normal braking= 94.69%, emergency braking = 100 ms	-	OM, RTM & RVM
Hekmatmanesh et al. [37] 2020	EEG	ERD/ERS	CSP,Variance filtered data and frequency spectral analysis	SSVM with GRBF kernel	S, B for moving forward and brake	OM= 92.70%, RTM = 83.21%	1.5 s	OM, RTM
Dindorf et al. [49] 2020	EMG	low pass filter: 15 Hz		-	EBS	-	240 ms	OM, RTM
Lu et al. [43] 2020	EEG and vehicle parameters	SSVEP	frequency domain	SVM	Slow down, speed up and Keep speed	84.93%	-	OM, RTM
Li et al. [44] 2020	EEG and vehicle parameters	SSVEP and HUD	frequency domain	SVM	L, R, and S for turn left right and go forward	94.02%	-	OM, RTM
Dindorf et al. [50] 2021	EEG, EMG, eye movement	EEG: 0.5 to 50 Hz, Alpha and Beta waves, EMG the same features in [49]	filtered data and frequency spectral analysis	-	EBS	-	240 ms	OM, RTM
Liu et al. [54] 2021	EEG and Lidar	SSVEP	FBCCA	Correlation	F BW L R	95.63%	-	OM, RTM
Fei et al. [47] 2021	EEG	HUD and patterns related to flashs of nine characters	semi-MIM	TSVM	-	85.00%	-	OM, RTM

L= Left, R= Right, S= Steering, BW= Backward B= Brake, RFM= Right Foot Movement, SIM= Self-Initiated Movement, ES= External Stimulus, RTM= Real-time Mode, OM= Offline Mode, POM= Pseudo-real-time Mode, RT= Response Time, SAM= Semi-Autonomous Mode, RVM= Real-Vehicle Mode.

TABLE 2. The BCAV review studies in the past 10 years.

Authors Year	Signal	Patterns	Features	Classifiers	Task and control commands	Average Accuracy	RT	Modes
Royer et al. [61] 2010	EEG	ERD/ERS	Cross-correlation, autoregressive spectral amplitude	Linear classifier	RH, LH, BH, rest for L,R,U,D movements	-	2.1 s	OM, RTM, RADM
Akce et al. [62] 2010	EEG with feedback camera	ERD/ERS	CSAP	HMM with belief propagation	Imaginary RH, LH for specifying a path for a fixed Wings	-	-	OM, RTM
Doud et al. [71] 2011	EEG with camera feedback	ERD/ERS	time-frequency PSD	Amplitude threshold of the mu band	RH, LH, BH, rest, thong, feet for TR, TL, F,BW, U, D	85%	-	OM-RLT, RADM
Kim et al. [69] 2014	EEG eye camera	EEG, eye features	EEG = power Eye = contour points between the pupil and iris	linear kernel-based SVM	9 points eye gazing for 8 directions U, D, L, R, FW, BW, TR, TL	OM = 91.67% RTM = 80%	eye tracker RT = 117 ms, EEG RT = 84 ms	OM, RTM
Shi et al. [72] 2015	eye tracker EEG, camera	ERD/ERS	improved cross-correlation mean, skewness kurtosis, minimum, maximum, standard deviation	LR	L, R and Idle for L, R, F and camera for obstacle avoidance	-	94.36%	OM, SAM
Coenen et al. [16] 2015	EEG, EOG	auditory imagination and spatial navigation mental task	frequency feature and regression	LR	hand joystick or foot button box movement for horizontal& Vertical movement	85.66%	-	OM, RTM
Kosmyna et al. [73], [74] 2015	EEG & EMG	ERD/ERS & facial patterns	FastICA, average	adaptive recurrent NN, KNN	L, R, L foot for TL, TR, D	about 75%	-	OM, RTM
Khan et al. [81] 2015	EEG, NIRS	ERD/ERS SSVEP	PSD of EEG and HbO and HbR for NIRS	LDA	6 Hz visual flickering of light and MI for U&D and Foreward	78.33%	-	OM
Lin et al. [80] 2015	EEG, EMG	EEG, EMG patterns based on facial gestures	preprocessed EEG, EMG	PCA	small, frown, right and left wink facial gestures for R, L, F, BW, U, D	-	-	OM
Zhang et al. [82] 2018	EEG, Google glass 14 external sensors	SSVEP	Fourier Transform coefficients	SVM with RBF	L, R, (both) feet, both hand movement, touch pad gesture, head posture for R, L, F, BW, U, D	97.10%	-	OM, RTM

U = Up, D = Down, F = Forward, BW = Backward, R = Rotation, L = Left, R = Right, C = clockwise, UC = Un-Clockwise, H = Horizental, V= vertical, HbO = oxygenated hemoglobin, HbR = deoxygenated hemoglobin, RADM = real-aerial drone mode, CSAP = common spatial analytic pattern, MNV = Minimum negative value.

many maintenance operations will be safer to carry out and their costs can be reduced, safety at work in hazardous conditions (e.g., provision of first aid in remote or dangerous locations) can be enhanced, and checking and guaranteeing the security of large areas and factories will be easier. Further, new solutions will facilitate, for instance, weather monitoring in inaccessible areas (mountains, pole areas) or the delivery of post.

TABLE 2. ***(Continued.)*** **The BCAV review studies in the past 10 years.**

Authors Year	Signal	Patterns	Features	Classifiers	Task and control commands	Average Accuracy	RT	Modes
Khan et al. [83] 2016	EEG, facial gestures, fNIRS, camera	SSVEP, EOG	mean of HbO changes, PSD, peak and skewness	LDA	L, R, eye movement, 6 Hz pattern for U,D, rotation stop (obstacle avoidance	NIRS = 86.66% IM = 87.13% EOG = 86.96% SSVEP = 87.20%	-	OM
Duarte et al. [75] 2017	EEG	μ waves	CSP	LDA	TR and TL	84.40%	-	OM, RTM
kryger et al. [77] 2017	EEG	IM of hand and wrist	-	-	U, D, L, R, Pitch and Roll	-	-	OM, RTM
Khan et al. [68] 2017	EEG, fNIRS	patterns related to mental arithmetic, mental counting, word formation, and mental rotation	EEG= number of peaks, skewness fNIRS = min, mean, HbO changes, skewness	LDA	U,D,F,R	84.00%	-	OM, RTM
Khan et al. [68] 2017	EEG, fNIRS	patterns related to mental arithmetic, mental counting, word formation, mental rotation in frontal, parietal, visual locations	EEG = number of peaks, skewness eye movements from EEG= mean, number of eye blinks, fNIRS = min, mean, HbO changes	LDA	L,R, eye movement from EEG, IM and fNIRS for U,D, F,BW, TR, TL, CR, UCR	fNIRS = 75.60% EEG = 86.00%	-	OM, RTM, RADM
Vishwanath et al. [76] 2018	EEG	filtered EEG	CSP	LDA for two classes nonlinera SVM for two classes	-	LDA: 85.84% nonliner SVM= 83.15%	-	OM, RTM
Zafar et al. [67] 2018	fNIRS	patterns related to mental arithmetic task	mean, slope, peak, changes of HbO and HbR, HbT and COE	SVM and VPA with Threshold circle	Mental arithmetic for F with constant speed	SVM =86%±5.40 VPA = 78%±8.30	2.3 s	OM, RTM, RADM
Zafar et al. [70] 2018	fNIRS	patterns related to mental arithmetic and mental counting tasks	mean, slope, peak, changes of HbO and HbR, HbT and COE	SVM and VPA with Threshold circle	mental arithmetic and mental counting F, U, R	74.00%	2.3 s	OM, RTM, RADM
Wang et al. [55] 2018	EEG, HMD	SSVEP	CCA	Threshold	flickering in different frequencies,for U, D, F and TR	78.00%	-	OM, RTM
Chiuzbaian et al. [78] 2019	EEG	SSVEP	Frequency Spectral Analysis	Frequency Threshold	U, D, R, L	-	-	OM, RTM
Kavichai et al. [84] 2019	EEG, fNIRS, distance measurement sensors, GPS	the same as Khan et al. [68]	SCS (combination of [68] with the external sensors and GPS)	the same as Khan et al. [68]	the same as Khan et al. [68] with GPS&external sensors for OAC	-	-	OM
Duan et al. [79] 2019	EEG	SSVEP, ERD/ERS, Eye Blink	C1-CSP, CCA, amplitude	Correlation	flickering different frequencies, for U, D, R, L	86.50%	-	OM, RTM
Chen et al. [85] 2020	EEG, EOG	ERD/ERS, Eye movement	EEG = CSP, EOG = DTCWT, Eye Blink, VEOG HEOG, Waveform features	SVM	U, D, F, BW, R, L	96.78%	-	OM, RTM
Kogava and Kar et al. [87]–[89] 2020-2021	Eye Tracker	Eye Movements	Eye position on a screen	-	U, D, F, L, R	-	-	OM
Kim et al. [86] 2021	EEG	ERD/ERS	CSP features power of Alpha	LDA, SVM, DT ,Ensemble	Hovering, Splitting, Dispersing, Aggregating	LDA = 76.4% ±4.2	-	OM
Kapgate [90] 2021	EEG	SSVEP, Alpha and Beta waves, p300	SSVEP = PSD of Alpha and Beta, p300 = filtered EEG between 0.1–12 Hz, CSP	LDA	U D F BW	88.00%	-	OM

U = Up, D = Down, F = Forward, BW = Backward, R = Rotation, L = Left, R = Right, C = clockwise, UC = Un-Clockwise, H = Horizental, V = vertical, HbO = oxygenated hemoglobin, HbR = deoxygenated hemoglobin, RADM = real-aerial drone mode, MNV = Minimum negative value.

APPENDIX

In this appendix, we provide a systematic presentation of the most significant literature in the topic of BCV and BCAV from the past ten years, presented in Tables 1 and 2 in the following pages, respectively.

REFERENCES

[1] A. Hekmatmanesh, V. Zhidchenko, K. Kauranen, K. Siitonen, H. Handroos, S. Soutukorva, and A. Kilpeläinen, "Biosignals in human factors research for heavy equipment operators: A review of available methods and their feasibility in laboratory and ambulatory studies," *IEEE Access*, vol. 9, pp. 97466–97482, 2021.

[2] H. Von Helmholtz, *Handbuch der Physiologischen Optik*. Wipperfürth, Germany: Voss, 1867, vol. 9.

[3] A. Hekmatmanesh, R. M. Asl, H. Wu, and H. Handroos, "EEG control of a bionic hand with imagination based on chaotic approximation of largest Lyapunov exponent: A single trial BCI application study," *IEEE Access*, vol. 7, pp. 105041–105053, 2019.

[4] J. Zhang and M. Wang, "A survey on robots controlled by motor imagery brain–computer interfaces," *Cogn. Robot.*, vol. 1, pp. 12–24, Jan. 2021.

[5] A. Hekmatmanesh, H. Wu, A. Motie-Nasrabadi, M. Li, and H. Handroos, "Combination of discrete wavelet packet transform with detrended fluctuation analysis using customized mother wavelet with the aim of an imagery-motor control interface for an exoskeleton," *Multimedia Tools Appl.*, vol. 78, pp. 30503–30522, May 2019.

[6] A. Hekmatmanesh, "Investigation of EEG signal processing for rehabilitation robot control," 2019.

[7] P. Stawicki, F. Gembler, and I. Volosyak, "Driving a semiautonomous mobile robotic car controlled by an SSVEP-based BCI," *Comput. Intell. Neurosci.*, vol. 2016, pp. 1–14, Mar. 2016.

[8] Y. Lu and L. Bi, "EEG signals-based longitudinal control system for a brain-controlled vehicle," *IEEE Trans. Neural Syst. Rehabil. Eng.*, vol. 27, no. 2, pp. 323–332, Feb. 2019.

[9] R. H. Abiyev, N. Akkaya, E. Aytac, I. Günsel, and A. Çağman, "Brain-computer interface for control of wheelchair using fuzzy neural networks," *BioMed Res. Int.*, vol. 2016, pp. 1–9, Sep. 2016.

[10] A. Cruz, G. Pires, A. Lopes, C. Carona, and U. J. Nunes, "A self-paced BCI with a collaborative controller for highly reliable wheelchair driving: Experimental tests with physically disabled individuals," *IEEE Trans. Human-Mach. Syst.*, vol. 51, no. 2, pp. 109–119, Apr. 2021.

[11] L. Bi, X.-A. Fan, and Y. Liu, "EEG-based brain-controlled mobile robots: A survey," *IEEE Trans. Human-Mach. Syst.*, vol. 43, no. 2, pp. 161–176, Mar. 2013.

[12] D. J. Crammond and J. F. Kalaska, "Prior information in motor and premotor cortex: Activity during the delay period and effect on pre-movement activity," *J. Neurophysiol.*, vol. 84, no. 2, pp. 986–1005, Aug. 2000.

[13] C. Neuper and W. Klimesch, *Event-Related Dynamics of Brain Oscillations*. Amsterdam, The Netherlands: Elsevier, 2006.

[14] E. M. Sokhadze, M. F. Casanova, E. L. Casanova, E. Lamina, D. P. Kelly, and I. Khachidze, "Event-related potentials (ERP) in cognitive neuroscience research and applications," *NeuroRegulation*, vol. 4, no. 1, p. 14, 2017.

[15] A. Kemp, M. A. Gray, P. Eide, R. Silberstein, and P. J. Nathan, "Steady-state visually evoked potential topography during processing of emotional valence in healthy subjects," *NeuroImage*, vol. 17, no. 4, pp. 1684–1692, Dec. 2002.

[16] J. Coenen, "UAV BCI comparison of manual and pedal control systems for 2D flight performance of users with simultaneous BCI control," 2015.

[17] H. H. Kornhuber and L. Deecke, "Hirnpotentialänderungen bei willkürbewegungen und passiven bewegungen des menschen: Bereitschaftspotential und reafferente potentiale," *Pflüger's Archiv für die Gesamte Physiologie des Menschen und der Tiere*, vol. 284, no. 1, pp. 1–17, 1965.

[18] C. H. Brunia, "CNV and SPN: Indices of anticipatory behavior," in *The Bereitschaftspotential*. Boston, MA, USA: Springer, 2003, pp. 207–227.

[19] N. Naseer and K.-S. Hong, "FNIRS-based brain-computer interfaces: A review," *Frontiers Hum. Neurosci.*, vol. 9, p. 3, Jan. 2015.

[20] R. Abreu, A. Leal, and P. Figueiredo, "EEG-informed fMRI: A review of data analysis methods," *Frontiers Hum. Neurosci.*, vol. 12, p. 29, Feb. 2018.

[21] D. Göhring, D. Latotzky, M. Wang, and R. Rojas, "Semi-autonomous car control using brain computer interfaces," in *Intelligent Autonomous Systems 12*. Berlin, Germany: Springer, 2013, pp. 393–408.

[22] L. Bi, H. Wang, T. Teng, and C. Guan, "A novel method of emergency situation detection for a brain-controlled vehicle by combining EEG signals with surrounding information," *IEEE Trans. Neural Syst. Rehabil. Eng.*, vol. 26, no. 10, pp. 1926–1934, Oct. 2018.

[23] H. Shah-Hosseini, "The intelligent water drops algorithm: A nature-inspired swarm-based optimization algorithm," *Int. J. Bio-Inspired Comput.*, vol. 1, nos. 1–2, pp. 71–79, 2009.

[24] A. Kaveh, "Optimum design of castellated beams using the tug of war algorithm," in *Applications of Metaheuristic Optimization Algorithms in Civil Engineering*. Cham, Switzerland: Springer, 2017, pp. 9–30.

[25] S. M. R. Noori, A. Hekmatmanesh, M. Mikaeili, and K. Sadeghniiat-Haghighi, "*K*-complex identification in sleep EEG using MELM-GRBF classifier," in *Proc. 21th Iranian Conf. Biomed. Eng. (ICBME)*, Nov. 2014, pp. 119–123.

[26] A. Hekmatmanesh, M. Mikaeili, K. Sadeghniiat-Haghighi, H. Wu, H. Handroos, R. Martinek, and H. Nazeran, "Sleep spindle detection and prediction using a mixture of time series and chaotic features," *Adv. Elect. Electron. Eng.*, vol. 15, no. 3, pp. 435–447, 2017.

[27] A. Hekmatmanesh, S. M. R. Noori, and M. Mikaili, "Sleep spindle detection using modified extreme learning machine generalized radial basis function method," in *Proc. 22nd Iranian Conf. Electr. Eng. (ICEE)*, May 2014, pp. 1898–1902.

[28] Y. Lu and L. Bi, "Combined lateral and longitudinal control of EEG signals-based brain-controlled vehicles," *IEEE Trans. Neural Syst. Rehabil. Eng.*, vol. 27, no. 9, pp. 1732–1742, Sep. 2019.

[29] A. Hekmatmanesh, H. Wu, M. Li, A. M. Nasrabadi, and H. Handroos, "Optimized mother wavelet in a combination of wavelet packet with detrended fluctuation analysis for controlling a remote vehicle with imagery movement: A brain computer interface study," in *New Trends in Medical and Service Robotics*. Cham, Switzerland: Springer, 2019, pp. 186–195.

[30] L. G. Hernández, O. M. Mozos, J. M. Ferrández, and J. M. Antelis, "EEG-based detection of braking intention under different car driving conditions," *Frontiers Neuroinform.*, vol. 12, p. 29, May 2018.

[31] J. Zhuang, K. Geng, and G. Yin, "Ensemble learning based brain-computer interface system for ground vehicle control," *IEEE Trans. Syst., Man, Cybern., Syst.*, early access, Dec. 9, 2019, doi: 10.1109/TSMC.2019.2955478.

[32] T. Teng, L. Bi, and Y. Liu, "EEG-based detection of driver emergency braking intention for brain-controlled vehicles," *IEEE Trans. Intell. Transp. Syst.*, vol. 19, no. 6, pp. 1766–1773, Jun. 2018.

[33] S. Haufe, M. S. Treder, M. F. Gugler, M. Sagebaum, G. Curio, and B. Blankertz, "EEG potentials predict upcoming emergency brakings during simulated driving," *J. Neural Eng.*, vol. 8, no. 5, 2011, Art. no. 056001.

[34] L. Bi, X.-A. Fan, K. Jie, T. Teng, H. Ding, and Y. Liu, "Using a head-up display-based steady-state visually evoked potential brain–computer interface to control a simulated vehicle," *IEEE Trans. Intell. Transp. Syst.*, vol. 15, no. 3, pp. 959–966, Jun. 2014.

[35] I.-H. Kim, J.-W. Kim, S. Haufe, and S.-W. Lee, "Detection of braking intention in diverse situations during simulated driving based on EEG feature combination," *J. Neural Eng.*, vol. 12, no. 1, 2014, Art. no. 016001.

[36] K. Fukunaga, *Introduction to Statistical Pattern Recognition*. Amsterdam, The Netherlands: Elsevier, 2013.

[37] A. Hekmatmanesh, H. Wu, F. Jamaloo, M. Li, and H. Handroos, "A combination of CSP-based method with soft margin SVM classifier and generalized RBF kernel for imagery-based brain computer interface applications," *Multimedia Tools Appl.*, vol. 79, pp. 17521–17549, Feb. 2020.

[38] A. Shakeel, M. S. Navid, M. N. Anwar, S. Mazhar, M. Jochumsen, and I. K. Niazi, "A review of techniques for detection of movement intention using movement-related cortical potentials," *Comput. Math. Methods Med.*, vol. 2015, pp. 1–13, Oct. 2015.

[39] S. Haufe, J.-W. Kim, I.-H. Kim, A. Sonnleitner, M. Schrauf, G. Curio, and B. Blankertz, "Electrophysiology-based detection of emergency braking intention in real-world driving," *J. Neural Eng.*, vol. 11, no. 5, 2014, Art. no. 056011.

[40] L. Bi, X.-A. Fan, N. Luo, K. Jie, Y. Li, and Y. Liu, "A head-up display-based P300 brain–computer interface for destination selection," *IEEE Trans. Intell. Transp. Syst.*, vol. 14, no. 4, pp. 1996–2001, Dec. 2013.

[41] X.-A. Fan, L. Bi, T. Teng, H. Ding, and Y. Liu, "A brain–computer interface-based vehicle destination selection system using P300 and SSVEP signals," *IEEE Trans. Intell. Transp. Syst.*, vol. 16, no. 1, pp. 274–283, Feb. 2015.

[42] L. Bi, Y. Lu, X. Fan, J. Lian, and Y. Liu, "Queuing network modeling of driver EEG signals-based steering control," *IEEE Trans. Neural Syst. Rehabil. Eng.*, vol. 25, no. 8, pp. 1117–1124, Aug. 2017.

[43] Y. Lu and L. Bi, "Human behavior model-based predictive control of longitudinal brain-controlled driving," *IEEE Trans. Intell. Transp. Syst.*, vol. 22, no. 3, pp. 1361–1374, Mar. 2021.

[44] H. Li, L. Bi, and J. Yi, "Sliding-mode nonlinear predictive control of brain-controlled mobile robots," *IEEE Trans. Cybern.*, early access, Nov. 24, 2020, doi: 10.1109/TCYB.2020.3031667.

[45] Y. Lu, L. Bi, and H. Li, "Model predictive-based shared control for brain-controlled driving," *IEEE Trans. Intell. Transp. Syst.*, vol. 21, no. 2, pp. 630–640, Feb. 2020.
[46] L. Bi, M. Wang, Y. Lu, and F. A. Genetu, "A shared controller for brain-controlled assistive vehicles," in *Proc. IEEE Int. Conf. Adv. Intell. Mechatronics (AIM)*, Jul. 2016, pp. 125–129.
[47] W. Fei, L. Bi, and J. Zhang, "Adaptive brain-machine interface of brain-controlled vehicles using semi-MIM and TSVM," in *Proc. 5th Int. Conf. Control Eng. Artif. Intell.*, Jan. 2021, pp. 31–35.
[48] T.-H. Nguyen and W.-Y. Chung, "Detection of driver braking intention using EEG signals during simulated driving," *Sensors*, vol. 19, no. 13, p. 2863, Jun. 2019.
[49] R. Dindorf and P. Wos, "Analysis of the possibilities of using a driver's brain activity to pneumatically actuate a secondary foot brake pedal," *Actuators*, vol. 9, no. 3, p. 49, 2020.
[50] R. Dindorf, J. Takosoglu, and P. Wos, "Study on a brain-controlled pneumatic actuator to assist emergency braking of a vehicle," *Commun., Sci. Lett. Univ. Zilina*, vol. 23, no. 3, pp. F49–F57, Jul. 2021.
[51] X. Zhao, S. Wang, J. Ma, Q. Yu, Q. Gao, and M. Yu, "Identification of driver's braking intention based on a hybrid model of GHMM and GGAP-RBFNN," *Neural Comput. Appl.*, vol. 31, no. S1, pp. 161–174, Jan. 2019.
[52] S. Wang, Q. Yu, and X. Zhao, "Study on driver's turning intention recognition hybrid model of GHMM and GGAP-RBF neural network," *Adv. Mech. Eng.*, vol. 10, no. 3, 2018, Art. no. 1687814018764985.
[53] B.-J. Yoon, "Hidden Markov models and their applications in biological sequence analysis," *Current Genomics*, vol. 10, no. 6, pp. 402–415, 2009.
[54] S. Liu, D. Zhang, M. Qiao, K. Wang, S. Zhao, Y. Yang, and T. Yan, "Mind controlled vehicle based on LiDAR SLAM navigation and SSVEP technology," in *Proc. 9th Int. Winter Conf. Brain-Comput. Interface (BCI)*, Feb. 2021, pp. 1–4.
[55] M. Wang, R. Li, R. Zhang, G. Li, and D. Zhang, "A wearable SSVEP-based BCI system for quadcopter control using head-mounted device," *IEEE Access*, vol. 6, pp. 26789–26798, 2018.
[56] A. Hekmatmanesh, F. Jamaloo, H. Wu, H. Handroos, and A. Kilpeläinen, "Common spatial pattern combined with kernel linear discriminate and generalized radial basis function for motor imagery-based brain computer interface applications," *AIP Conf. Proc.*, vol. 1956, no. 1, 2018, Art. no. 020003.
[57] A. Hekmatmanesh, R. M. Asl, H. Handroos, and H. Wu, "Optimizing largest Lyapunov exponent utilizing an intelligent water drop algorithm: A brain computer interface study," in *Proc. 5th Int. Conf. Event-Based Control, Commun., Signal Process. (EBCCSP)*, May 2019, pp. 1–5.
[58] H. Zhang, R. Chavarriaga, Z. Khaliliardali, L. Gheorghe, I. Iturrate, and J. D. R. Millán, "EEG-based decoding of error-related brain activity in a real-world driving task," *J. Neural Eng.*, vol. 12, no. 6, Dec. 2015, Art. no. 066028.
[59] L. Yang, R. Ma, H. M. Zhang, W. Guan, and S. Jiang, "Driving behavior recognition using EEG data from a simulated car-following experiment," *Accident Anal. Prevention*, vol. 116, pp. 30–40, Jul. 2018.
[60] A. Nourmohammadi, M. Jafari, and T. O. Zander, "A survey on unmanned aerial vehicle remote control using brain–computer interface," *IEEE Trans. Human-Mach. Syst.*, vol. 48, no. 4, pp. 337–348, Aug. 2018.
[61] A. S. Royer, A. J. Doud, M. L. Rose, and B. He, "EEG control of a virtual helicopter in 3-dimensional space using intelligent control strategies," *IEEE Trans. Neural Syst. Rehabil. Eng.*, vol. 18, no. 6, pp. 581–589, Dec. 2010.
[62] A. Akce, M. Johnson, and T. Bretl, "Remote teleoperation of an unmanned aircraft with a brain-machine interface: Theory and preliminary results," in *Proc. IEEE Int. Conf. Robot. Autom.*, May 2010, pp. 5322–5327.
[63] K. LaFleur, K. Cassady, A. Doud, K. Shades, E. Rogin, and B. He, "Quadcopter control in three-dimensional space using a noninvasive motor imagery-based brain–computer interface," *J. Neural Eng.*, vol. 10, no. 4, 2013, Art. no. 046003.
[64] B. Z. Allison, S. Dunne, R. Leeb, J. D. R. Millán, and A. Nijholt, *Towards Practical Brain-Computer Interfaces: Bridging the Gap From Research to Real-World Applications*. Springer, 2012.
[65] R. Chaurasia and V. Mohindru, "Unmanned aerial vehicle (UAV): A comprehensive survey," in *Unmanned Aerial Vehicles for Internet of Things (IoT): Concepts, Techniques, and Applications*. Hoboken, NJ, USA: Wiley, 2021, p. 1.
[66] R. Naveen and G. Sivaraj, "Mind-controlled unmanned aerial vehicle (UAV) using brain–computer interface (BCI)," in *Unmanned Aerial Vehicles for Internet of Things (IoT): Concepts, Techniques, and Applications*. Hoboken, NJ, USA: Wiley, 2021, p. 231.
[67] A. Zafar, U. Ghafoor, M. J. Khan, and K.-S. Hong, "Drone control using functional near-infrared spectroscopy," in *Proc. 15th Int. Conf. Electr. Eng./Electron., Comput., Telecommun. Inf. Technol. (ECTI-CON)*, Jul. 2018, pp. 384–387.
[68] M. J. Khan and K.-S. Hong, "Hybrid EEG–fNIRS-based eight-command decoding for BCI: Application to quadcopter control," *Frontiers Neurorobot.*, vol. 11, p. 6, Feb. 2017.
[69] B. H. Kim, M. Kim, and S. Jo, "Quadcopter flight control using a low-cost hybrid interface with EEG-based classification and eye tracking," *Comput. Biol. Med.*, vol. 51, pp. 82–92, Aug. 2014.
[70] A. Zafar, M. J. Khan, J. Park, and K.-S. Hong, "Initial-dip based quadcopter control: Application to fNIRS-BCI," *IFAC-PapersOnLine*, vol. 51, no. 15, pp. 945–950, 2018.
[71] A. J. Doud, J. P. Lucas, M. T. Pisansky, and B. He, "Continuous three-dimensional control of a virtual helicopter using a motor imagery based brain-computer interface," *PLoS ONE*, vol. 6, no. 10, Oct. 2011, Art. no. e26322.
[72] T. Shi, H. Wang, and C. Zhang, "Brain Computer Interface system based on indoor semi-autonomous navigation and motor imagery for unmanned aerial vehicle control," *Expert Syst. Appl.*, vol. 42, no. 9, pp. 4196–4206, 2015.
[73] N. Kosmyna, F. Tarpin-Bernard, and B. Rivet, "Towards brain computer interfaces for recreational activities: Piloting a drone," in *Proc. IFIP Conf. Hum.-Comput. Interact.* Cham, Switzerland: Springer, 2015, pp. 506–522.
[74] N. Kosmyna, F. Tarpin-Bernard, and B. Rivet, "Adding human learning in brain-computer interfaces (BCIs): Towards a practical control modality," *ACM Trans. Comput.-Hum. Interact.*, vol. 22, no. 3, pp. 1–37, Jun. 2015.
[75] R. M. Duarte *et al.*, "Low cost brain computer interface system for AR.Drone control," M.S. thesis, 2017.
[76] R. M. Vishwanath, S. Kumaar, and S. N Omkar, "A real-time control approach for unmanned aerial vehicles using brain-computer interface," 2018, *arXiv:1809.00346*. [Online]. Available: http://arxiv.org/abs/1809.00346
[77] M. Kryger, B. Wester, E. A. Pohlmeyer, M. Rich, B. John, J. Beaty, M. McLoughlin, M. Boninger, and E. C. Tyler-Kabara, "Flight simulation using a brain-computer interface: A pilot, pilot study," *Exp. Neurol.*, vol. 287, pp. 473–478, Jan. 2017.
[78] A. Chiuzbaian, J. Jakobsen, and S. Puthusserypady, "Mind controlled drone: An innovative multiclass SSVEP based brain computer interface," in *Proc. 7th Int. Winter Conf. Brain-Comput. Interface (BCI)*, Feb. 2019, pp. 1–5.
[79] X. Duan, S. Xie, X. Xie, Y. Meng, and Z. Xu, "Quadcopter flight control using a non-invasive multi-modal brain computer interface," *Frontiers Neurorobot.*, vol. 13, p. 23, May 2019.
[80] J.-S. Lin and Z.-Y. Jiang, "Implementing remote presence using quadcopter control by a non-invasive BCI device," *Comput. Sci. Inf. Technol.*, vol. 3, no. 4, pp. 122–126, 2015.
[81] M. J. Khan, K.-S. Hong, N. Naseer, and M. R. Bhutta, "Hybrid EEG-NIRS based BCI for quadcopter control," in *Proc. 54th Annu. Conf. Soc. Instrum. Control Eng. Jpn. (SICE)*, Jul. 2015, pp. 1177–1182.
[82] M. M. Jackson, "Quadcopter navigation using Google glass and braincomputer interface," 2015.
[83] M. J. Khan, A. Zafar, and K.-S. Hong, "Hybrid EEG-NIRS based active command generation for quadcopter movement control," in *Proc. Int. Autom. Control Conf. (CACS)*, Nov. 2016, pp. 200–205.
[84] E. Kavichai, R. Huang, and S.-W. Woo, "Shared control strategies for BCI-based quadcopter control," in *Proc. 16th Int. Conf. Electr. Eng./Electron., Comput., Telecommun. Inf. Technol. (ECTI-CON)*, Jul. 2019, pp. 155–158.
[85] C. Chen, P. Zhou, A. N. Belkacem, L. Lu, R. Xu, X. Wang, W. Tan, Z. Qiao, P. Li, Q. Gao, and D. Shin, "Quadcopter robot control based on hybrid brain–computer interface system," *Sensors Mater.*, vol. 32, no. 3, pp. 991–1004, 2020.
[86] S.-J. Kim, B.-H. Kwon, and J.-H. Jeong, "Intuitive visual imagery decoding for drone swarm formation control from EEG signals," in *Proc. 9th Int. Winter Conf. Brain-Comput. Interface (BCI)*, Feb. 2021, pp. 1–6.
[87] A. Kogawa, M. Onda, Y. Kai, T. Tanioka, Y. Yasuhara, and H. Ito, "Development of a remote-controlled drone system by using only eye movements for bedridden patients," in *Proc. Symp. Robot Design, Dyn. Control*. Cham, Switzerland: Springer, 2020, pp. 92–99.
[88] A. Kogawa, M. Onda, and Y. Kai, "Development of a remote-controlled drone system by using only eye movements: Design of a control screen considering operability and microsaccades," *J. Robot. Mechatron.*, vol. 33, no. 2, pp. 301–312, Apr. 2021.

[89] Y. Kai, H. M. U. Munir, M. Onda, Y. Adachi, J. Hayama, Y. Zhao, T. Tanioka, R. Locsin, K. Takase, and M. J. S. Dino, "Evaluation of the remote-controlled drone system using an eye-tracking device through the internet for patients in bedridden conditions," *Enfermería Clínica*, vol. 30, pp. 18–22, Feb. 2020.

[90] D. Kapgate, "Efficient quadcopter flight control using hybrid SSVEP + P300 visual brain computer interface," *Int. J. Hum.–Comput. Interact.*, pp. 1–11, 2021.

[91] R. C. Moioli, P. H. J. Nardelli, M. T. Barros, W. Saad, A. Hekmatmanesh, P. E. G. Silva, A. S. de Sena, M. Dzaferagic, H. Siljak, W. Van Leekwijck, D. Carrillo, and S. Latre, "Neurosciences and wireless networks: The potential of brain-type communications and their applications," *IEEE Commun. Surveys Tuts.*, early access, Jun. 23, 2021, doi: 10.1109/COMST.2021.3090778.

[92] A. Singandhupe, H. M. La, and D. Feil-Seifer, "Reliable security algorithm for drones using individual characteristics from an EEG signal," *IEEE Access*, vol. 6, pp. 22976–22986, 2018.

[93] J. Park, J. Park, D. Shin, and Y. Choi, "A BCI based alerting system for attention recovery of UAV operators," *Sensors*, vol. 21, no. 7, p. 2447, Apr. 2021.

[94] L. Giraudet, J.-P. Imbert, M. Bérenger, S. Tremblay, and M. Causse, "'The neuroergonomic evaluation of human machine interface design in air traffic control using behavioral and EEG/ERP measures': Erratum," 2016.

[95] H. Wang, L. Bi, and T. Teng, "EEG-based emergency braking intention prediction for brain-controlled driving considering one electrode falling-off," in *Proc. 39th Annu. Int. Conf. IEEE Eng. Med. Biol. Soc. (EMBC)*, Jul. 2017, pp. 2494–2497.

AMIN HEKMATMANESH received the bachelor's degree in electrical engineering from the Science and Research of Fars University, Shiraz, Iran, in 2010, the master's degree in biomedical engineering from Shahed University, Tehran, Iran, in 2013, and the Ph.D. degree in brain-controlled ankle foot and hand orthosis and control of mobile vehicle robots using imaginary movements based on the EEG from the Laboratory of Intelligent Machines, Lappeenranta University of Technology, in 2019. His master's thesis was about analyzing sleep EEG signal processing, memory consolidation, learning and negative emotional memory. Since 2020, he has been holding a postdoctoral position in heavy machine operator's health monitoring and signal processing for simulators with the Laboratory of Intelligent Machines, Lappeenranta University of Technology.

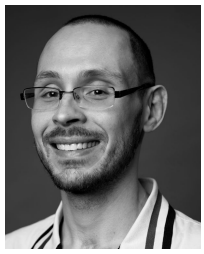

PEDRO H. J. NARDELLI (Senior Member, IEEE) received the B.S. and M.Sc. degrees in electrical engineering from the State University of Campinas, Brazil, in 2006 and 2008, respectively, and the Ph.D. degree from the University of Oulu, Finland, and State University of Campinas following a dual degree agreement, in 2013. He is currently an Associate Professor (Tenure Track) in IoT in energy systems with LUT University, Finland, and holds a position of Academy of Finland Research Fellow with a project called Building the Energy Internet as a large-scale IoT-based cyber-physical system that manages the energy inventory of distribution grids as discretized packets via machine-type communications (EnergyNet). He leads the Cyber-Physical Systems Group, LUT. He is a Project Coordinator of the CHIST-ERA European consortium Framework for the Identification of Rare Events via Machine Learning and IoT Networks (FIREMAN) and of the project Swarming Technology for Reliable and Energy-aware Aerial Missions (STREAM) supported by Jane and Aatos Erkko Foundation. He is also Docent at University of Oulu in the topic of communications strategies and information processing in energy systems. His research interest includes wireless communications particularly applied in industrial automation and energy systems.

HEIKKI HANDROOS (Member, IEEE) received the M.Sc. (Eng.) and D.Sc. (Tech.) degrees from Tampere University of Technology, in 1985 and 1991, respectively. Since 1992, he has been a Professor of machine automation with Lappeenranta University of Technology. He has been a Visiting Professor with the University of Minnesota, Peter the Great St. Petersburg Polytechnic University, and the National Defense Academy, Japan. He has led several important domestic and international research project. He has published about 250 international scientific articles and supervised around 20 D.Sc. (Tech.) theses. His research interests include modeling, design, and control of mechatronic transmissions to robotics and virtual engineering. Since 2014, he has been an Associate Editor of *Journal of Dynamic Systems, Measurement, and Control* (ASME).